[redacted]

MARTIN MARIETTA ENERGY SYSYEMS LIBRARIES
3 4456 0323401 5

writers

CENTRAL RESEARCH LIBRARY
DOCUMENT COLLECTION

ORNL 1794
VOLUME II

AEC RESEARCH AND DEVELOPMENT REPORT

THE OAK RIDGE NATIONAL LABORATORY

RESEARCH REACTOR SAFEGUARD REPORT

VOLUME II – APPENDIX

F. T. Binford
Editor

OAK RIDGE NATIONAL LABORATORY
CENTRAL RESEARCH LIBRARY
CIRCULATION SECTION
4500N ROOM 175
LIBRARY LOAN COPY
DO NOT TRANSFER TO ANOTHER PERSON
If you wish someone else to see this report, send in name with report and the library will arrange a loan.
UCN-7969 (3 9-77)

DECLASSIFIED
CLASSIFICATION CHANGED TO:
BY AUTHORITY OF: AEC 3-13-63
BY: J. Bradley 3-12-64

OAK RIDGE NATIONAL LABORATORY
OPERATED BY
CARBIDE AND CARBON CHEMICALS COMPANY
A DIVISION OF UNION CARBIDE AND CARBON CORPORATION
UCC
POST OFFICE BOX P
OAK RIDGE, TENNESSEE

[redacted]

[redacted]

[redacted]

[redacted]

ORNL 1794
VOLUME II

This document consists of 102 pages.

Copy 35 of 41 copies. Series A.

Contract No. W-7405-eng26

THE OAK RIDGE NATIONAL LABORATORY RESEARCH REACTOR

SAFEGUARD REPORT

VOLUME II APPENDIX

Research Reactor Design Group
F. T. Binford, Report Editor
T. E. Cole, Chairman, Steering Committee
J. P. Gill, Project Engineer

DATE ISSUED

OCT 7 1954

OAK RIDGE NATIONAL LABORATORY
Operated by
CARBIDE AND CARBON CHEMICALS COMPANY
A Division of Union Carbide and Carbon Corporation
Post Office Box P
Oak Ridge, Tennessee

[redacted]

[redacted]

MARTIN MARIETTA ENERGY SYSYEMS LIBRARIES

3 4456 0323401 5

[redacted]

[redacted]

FORWARD

This appendix consists of a collection of documents which are presented not only in support of the conclusions reached in Volume I of this report, but also for the purpose of establishing a reference volume for future use in connection with reactors of similar design.

The various sections of this volume, for the most part, reproduce individual reports and studies which have been made for the purpose of completing the design of the ORR.

[redacted]

[redacted]

TABLE OF CONTENTS

APPENDIX		PAGE
a	Nuclear Specifications of the ORR	1
b	ORR Shielding Studies I Basic Design Information	3
c	Activity Present in the Cooling System of the ORR	19
d	Estimate of the Shielding Figured for Pipelines Carrying N^{16} Bearing Water	24
e	Estimate of the Radiation Intensity at the ORR Cooling Loop Heat Exhangers	29
f	An Estimate of the Contribution to the Radiation Intensity above the Surface of the Research Reactor Due to the Presence of N^{16}	30
g	Operating Conditions of the ORR Cooling System	46
h	The Experiment Review Committee	56
i	Reactor Operation Review Committee	57
j	Radioisotope Production in the ORR	58
k	Proposed ANP Experiments in the ORR	63
l	Reactor Mechanical Controls	65
m	Dispersion of Airborne Wastes in the X-10 Area	69
n	Make up of Surrounding Area	87
o	Selected Radiation Hazards of ORR	93

[redacted] [redacted]

INDEX OF FIGURES

	Page
Particle Fluxes for Laboratory Tolerances	13
Dose Buildup Factor for Point Source-Water	14
Dose Buildup Factor for Point Source-Aluminum	15
Dose Buildup Factor for Point Source-Lead	16
Linear Absorbtion Coefficient for Photons in Barytes Concrete	17
Linear Absorbtion Coefficent for Photons in Ordinary Concrete	18
Demineralizer Effectiveness vs Fractional Flow	22
Concrete Shield Thickness Required to Reduce Radiation from Pipelines	25
Shield Thickness vs Radiation Intensity for Barytes Concrete Ceiling	28
ORR Fuel Assembly Maximum Surface Temperature - 10 MW	51
ORR Fuel Assembly Maximum Surface Temperature - 5 MW	52
ORR Mechanical Control System	67
Shim Rod Release Mechanism	68
Distribution of Temperature Gradient 1949-1950	71
Low Level Soundings 1949-1950	72
Annual Frequency of Wind Distribution	74
Annual Wind Roses	76
Effect of Parameters on Local Winds	79
Effect of Parameters on Local Winds	80
Annual Wind Roses for Knoxville and Nashville	84
Map of Counties Surrounding Oak Ridge Area	88

[redacted] [redacted]

APPENDIX a

NUCLEAR SPECIFICATIONS FOR THE ORR

TYPE: Modified MTR

POWER:
- INITIAL: Five Megawatts
- NOMINAL: Five - Ten Megawatts

FUEL: Enriched U^{235}

FUEL ELEMENTS: Alclad Sandwich Type
19 plates per element 24"x3"x0.05"

GRID SIZE: 9 elements x 7 elements

NUMBER OF ELEMENTS:
- NOMINAL: 28 (including 4 control-fuel rods)
- MAXIMUM: 33 (including 4 control-fuel rods)

MINIMUM CRITICAL MASS: 1680 grams (clean cold)

FLUX:	5 Megawatts	10 Megawatts
MAXIMUM VIRGIN nv	2.5×10^{13}	5×10^{13}
MAXIMUM EPITHERMAL	1×10^{14}	2×10^{14}
MAXIMUM THERMAL nv	8×10^{13}	1.6×10^{14}
AVERAGE THERMAL nv	5.7×10^{13}	1.14×10^{14}

REFLECTOR: Beryllium 3"-6"

MODERATOR: Demineralized Water

COOLANT: Demineralized Water

CONTROL AND SAFETY RODS: Cadmium-Fuel (Four with Positions for 12)

[redacted]

[redacted]

APPENDIX a

REACTIVITY REQUIREMENTS: (Over cold clean.)	5 Megawatts	10 Megawatts
TEMPERATURE COEFFICIENT:	0.8%	0.8%
FUEL BURNOUT:	2 %	2 %
EQUILIBRIUM XENON POISONING:	3.5%	3.8%
XENON POISONING OVERIDE:	14.5%	not considered(1)
EXPERIMENTS:(2)	5 %	5 %
TOTAL	15.8%	-

REACTIVITY EQUIVILENCE:

CONTROL RODS:	~8% each	~Total 34%
ENGINEERING TEST FACILITIES(3)	~1.4% each	~Total 2.8%
BEAM HOLES & EXPERIMENTS(3)		~Total 2.2%

DESIGN RADIATION LEVEL: 1/10 tolerance in working areas

(1) At some power level in excess of 5 megawatts it will become impractical to maintain sufficient excess reactivity to provide full Xenon overide.

(2) Strictly speaking the reactivity required to support the experiments should not be considered to be excess reactivity, since for any given case the reactor will be loaded only to the extent required to support the experiments to be performed.

(3) Experimental Values

[redacted]

[redacted]

APPENDIX b

ORR SHIELDING STUDIES
I - BASIC DESIGN INFORMATION

N. F. Lansing

Abstract

This memorandum sets forth a recommended uniform basis for designing the ORR shield. This includes design values for power level and emergent radiation, standard values for various material properties, and basic radiation intensities.

Introduction

In order to put all shielding and related studies for the ORR on a uniform basis, it is necessary that the various contributors employ a common body of physical properties and similar quantitative information. This will make comparison of results more meaningful than if each study is based on a more or less different set of postulates and properties.

Insofar as possible, these design bases employ the experimental shielding information which is now available. Also use has been made where appropriate, of some improved theoretical results - e.g., the tabulated build-up factors as published in the Reactor Handbook.

Basic Design Criteria

1. Reactor Power Level

The ORR system is to be designed for initial constant-power operation at 5 megawatts. However, radiation shielding is to provide throughout for steady operation at 30 megawatts.

2. Radiation Tolerance

Except for the immediate neighborhood of the large experimental facilities, the total emergent radiation penetrating the bulk shielding -- either the beam hole region or the pool wall-- is not to exceed 1/10 human tolerance. This intensity -- 0.75 mrem/hr -- must include

APPENDIX b

the combined effects of all radiations. The currently accepted particle fluxes for 1/10 tolerance* doses are compiled in Table I and presented graphically in Figure 1.

The general radiation level in the sub-pile room is not to exceed 30 mrem/hr for reactor operation at 30 mw. Somewhat higher radiation levels may be permitted in small portions of the sub-pile room provided that (a) the regions are sufficiently well defined that they can be isolated and (b) that it is not anticipated that frequent access to such regions will be required during normal operation.

Tentatively it is recommended that radiation levels at the top surface of the reactor pool not exceed tolerance (60 mrem/ 8-hr day). This is subject to revision following analysis of the effects of such a radiation source on the radiation intensities elsewhere around the reactor.

---

*This level, which may be termed "laboratory tolerance", represents not only some concession to experimentalists but also recognition that tolerance levels have been diminishing steadily during the past decade, and may conceivably again be reduced. It is not to be confused with a true "instrument tolerance" or reduction to natural background. This would require, according to P. R. Bell, that the radiation levels not exceed:

15 gamma-rays/(sq. cm) (sec) for photon energies of 100 kev or more

3 thermal neutrons/(sq. cm)(sec)

3 to 15 fast neutrons/(sq. cm)(sec)

APPENDIX b

3. Gamma-Ray Absorption Coefficients and Relaxation Lengths

These material properties have two distinctly different applications: (a) calculation of the attenuation of radiation for biological and similar shielding and (b) determination of the local energy-deposition rate, which is the magnitude of the thermal source, in order to be able to predict the temperature distribution in the structure.

For the attenuation calculation, it is customary to use the total absorption coefficient together with a build-up factor to calculate the transmission. For the thermal source, the local radiation intensity is based on the total cross-section and build-up factor combination but the absorption is given by the product of the intensity and the "energy-absorption" coefficient, μ_a.

Working values of both total and energy-absorption coefficients for a number of materials are compiled in Tables II and III. The inverse values, or relaxation lengths, are also given. For convenience, the entries are given for each of several length units.

In each case, conservative values have been chosen - i.e., values giving an upper limit either to transmission or to absorption as the case may be. For transmission calculations, the coefficients chosen are all minimum values within the range of gamma-ray energies expected (up to about 8 Mev). After studying the gamma-ray spectra obtained by Maienschein and others in the BSF, the energy

APPENDIX b

absorption coefficients have been chosen at 0.5 Mev. Although the center-line measurements reveal a peak around 2.2 Mev for reactor gamma-ray filtered by 100 cm or more of water, both the core emission spectrum and some off-centerline filtered spectra indicate that the softer components predominate in such cases. Because gamma-ray heating is of such significance in the design of many reactor core components, these somewhat conservative values are recommended.

4. Build-Up Factor

Although the NBS-NDA program has yielded gamma-ray build-up factors for water as well as for some elemental substances, there is as yet no equally well established compilation for such mixtures as concrete. Nevertheless, the necessities of proceeding with the design require that some choice be made, however arbitrary. Therefore, two "recipes" are recommended, on the basis of experience, as being both somewhat conservative and of a simple nature.

a. For analysis of attenuation by a given amount of material, it is recommended that the gamma-ray build-up factor be chosen equal to the number of relaxation lengths in terms of the total absorption coefficient - e.g., the values assembled in Table II.

b. For prediction of the required shielding to cause a certain attenuation, it is more convenient to set the build-up factor equal to exp $(0.17\mu_t x)$, Where x = shield thickness.

For convenience, some of the dose build-up factors as tabulated by Goldstein in the Reactor Handbook are presented graphically in Figures 2,3,4, and 5. The simple recipes are also shown for comparsion.

APPENDIX b

5. Radiation Intensities

At any point in the water outside the reactor tank, the radiation intensity is to be taken from the BSR work sheet (ORNL Dwg. 13769) for a distance equal to that between the given point in the ORR and the center of the face of the nearest possible reactor loading.

A recent recalibration, as reported in CF 53-5-21, indicates that the work sheet values are to be adjusted as follows:

Multiply values for	gamma-rays	0.8306
	fast neutrons	by 0.8306
	thermal neutrons	0.925

respectively.

For distances from the reactor face greater than 4 feet, these center-line data for radiation from a bare reactor apparently are good approximations to the off-center line intensities if distances are measured from the center of the reactor face. In other words, the radiation field varies more or less like the field from a point source located at the center of the reactor face.

In applying these data, allowance may be made for gamma-ray attenuation by the tank and other structural material provided that 1 foot of water is interposed between the reactor face and the structure. The neutron absorption by this water so reduces the neutron flux that (a) the capture gamma-rays from the structure are insignificant, and (b) the gamma-rays from neutron captures in water are virtually all subject to the same attenuation as those from the core.

In assessing the effect of a 3-inch (one element) thick beryllium reflector on the source strength, the following adjustments to the BSR data are recommended:

a. Distance are to be measured from the outer face of the reflector.

b. The fast neutrons are reduced by 1/3.

c. The gamma-rays are reduced by 1/1.3.

d. The thermal neutron flux is the same as given by the BSR work sheet. This in turn requires one foot of water between outer surface of the beryllium and structure whose gamma-ray attenuation is to be considered, due to the neutron capture gamma-ray effects outlined in the preceeding paragraph.

6. Permissible Temperature Difference in Concrete

For preliminary design purposes, the classical limit of 50°F permissible maximum temperature difference within the concrete is to be taken. This temperature difference is to include effects of ambient temperatures as well as the results of any internal heat generation.

7. Thermal and Mechanical Properties of Materials

Certain physical properties which enter the calculation of thermal stresses or which otherwise bear on the design of the shield are compiled here so that standard values may be employed in such calculations. These values are assembled in Table IV.

APPENDIX b

TABLE I

Energy Dependence of Neutron and Photon Fluxes

For Laboratory Tolerance (6.0 mrem/8-hr. day)*

Energy	Photons/(sq.cm)(sec)	Neutrons/(sq.cm)(sec)
Thermal	----	180
0.1 Mev	4800	134
0.2	2070	68
0.5	743	48
1	396	33
2	236	24
3	187	20
4	143	19
5	122	18
6	106	17
7	94	17
8	87	17
10	72	17

*Calculated from formulas prepared by K. Z. Morgan as given by M. S. Fair in Table 2.2.1 of the Reactor Handbook, Vol I (RH-1).

APPENDIX b

TABLE II

Gamma Ray Attenuation Characteristics

Total Absorption Coefficients

Materials	Absorption Coefficient, μ_t			Relaxation Length, λ_t		
	cm^{-1}	in^{-1}	ft^{-1}	cm	in	ft
Lead [a)]	0.481	1.24	14.9	2.08	0.805	0.0674
Ordinary concrete [b)]	0.0666	0.167	2.03	15	5.9	0.491
Barytes concrete [c)]	0.100	0.254	3.04	10	3.94	0.328
Aluminum [d)]	0.069	0.175	2.10	14.5	5.71	0.475
Water [e)]	0.0426	0.108	1.30	23.4	9.2	0.766

a. Based on total cross-section minimum value (at 3 Mev).

b. Based on asymptotic value from ORNL-414.

c. Extrapolated from ordinary concrete on density basis; also supported by calculation of μ_t as function of energy.

d. Based on total cross-section at 7 Mev. Value chosen for maximum energy gamma-rays of significant number.

e. Relaxation length about 150 cm from reactor surface according to BSF work sheet (ORNL Dwg. 13769).

APPENDIX b

TABLE III

Gamma-Ray Energy-Absorption Characteristics

Energy Absorption Coefficients*

Materials	μa, Absorption Coefficient			λa, Relaxation Length		
	cm^{-1}	in^{-1}	ft^{-1}	cm	in	ft
Lead	1.4	3.56	42.6	0.714	0.281	0.0234
Ordinary Concrete	0.057	0.145	1.74	17.5	6.91	0.575
Barytes Concrete	0.14	0.356	4.24	7.14	2.81	0.234
Aluminum	0.078	0.198	2.37	12.8	5.05	0.420
Steel	0.236	0.60	7.21	4.24	1.67	0.139
Cadmium	0.346	0.89	10.7	2.86	1.13	.0940
Uranium	3.0	7.60	91.5	0.33	0.13	1.0108
Beryllium	0.055	0.14	1.68	18.2	7.18	0.596
Water	0.033	0.084	1.00	30	11.8	0.985
Graphite	0.051	0.130	1.56	19.6	7.75	0.642

Chosen at or near 0.5 Mev from curves by Powell and Snyder (ORNL Dwg. 8117 R1, 8118 R1.)

APPENDIX b

Table IV

Thermal and Mechanical Properties of Shielding Materials

Material[a]	Thermal Conductivity, k $\frac{BTU}{(hr)(sq\ ft)(F/ft)}$	Thermal Expansion Coefficient, α ($F^{-1} \times 10^6$)	Modulus of Elasticity, E [lb/(sq. in.)] $\times 10^6$	Density, ρ (gm/cc)	Strength (psi)	Poisson's Ratio, ν
Aluminum						
2S	128	13.1	10	2.71	5000T	0.33
3S	111	12.9	10	2.73	6000T	0.33
356-T6	87	11.9	10.3	2.63	24000T	0.33
63S-T5	121	13.0	10	2.70	25000T	0.33
56S-0	68	13.5	10.3	2.64	22000T	0.33
Boral[b]	25			2.53	5500T 8240S	
Ordinary Concrete	0.54[c]	6	3.6	2.3	3500C	
Barytes Concrete	0.6[d]	10	5.3[e]	3.5	3500C	0.29[e]
Lead	20	16	2.4[f]	11.3	1600T	0.43[f]

(a) "Alcoa Aluminum and Its Alloys" (1947 ed.)
(b) ORNL 981
(c) Widely quoted value less than that reported in ORNL 1414. Chosen here as conservative.
(d) Lower limit cited in ORNL 1414 for barytes concrete with very small water content.
(e) Maximum values reported from Bureau of Reclamation tests on p. 156 of IDO-24003.
(f) Table 23, Section 1, "Handbook of Engineering Fundamentals", O. Eshbach. (1st Ed.)

Fig. 1 ORNL-LR-DWG. 2278

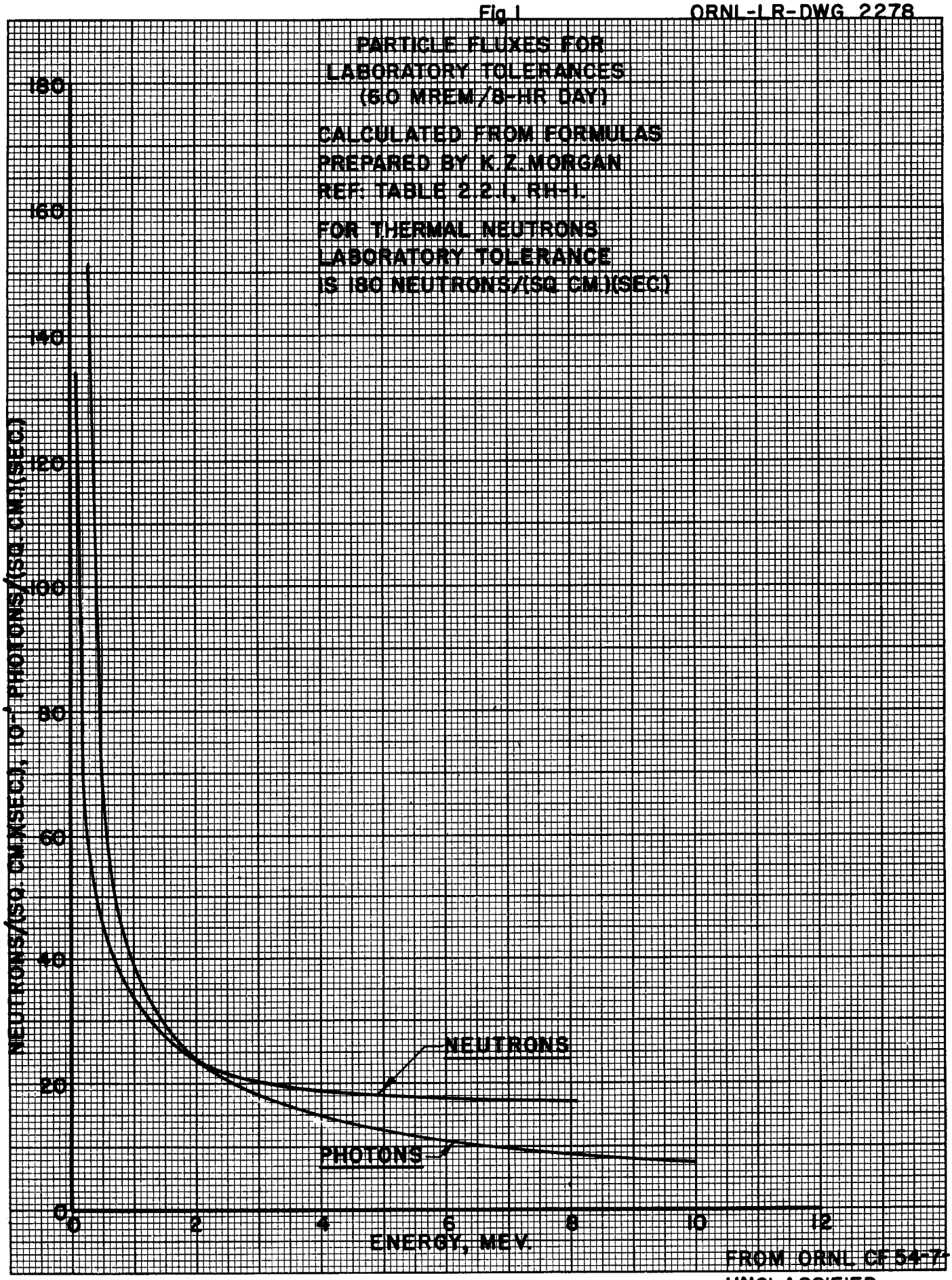

FROM ORNL CF 54-7-95
UNCLASSIFIED

Fig. 2

ORNL-LR-DWG-2268

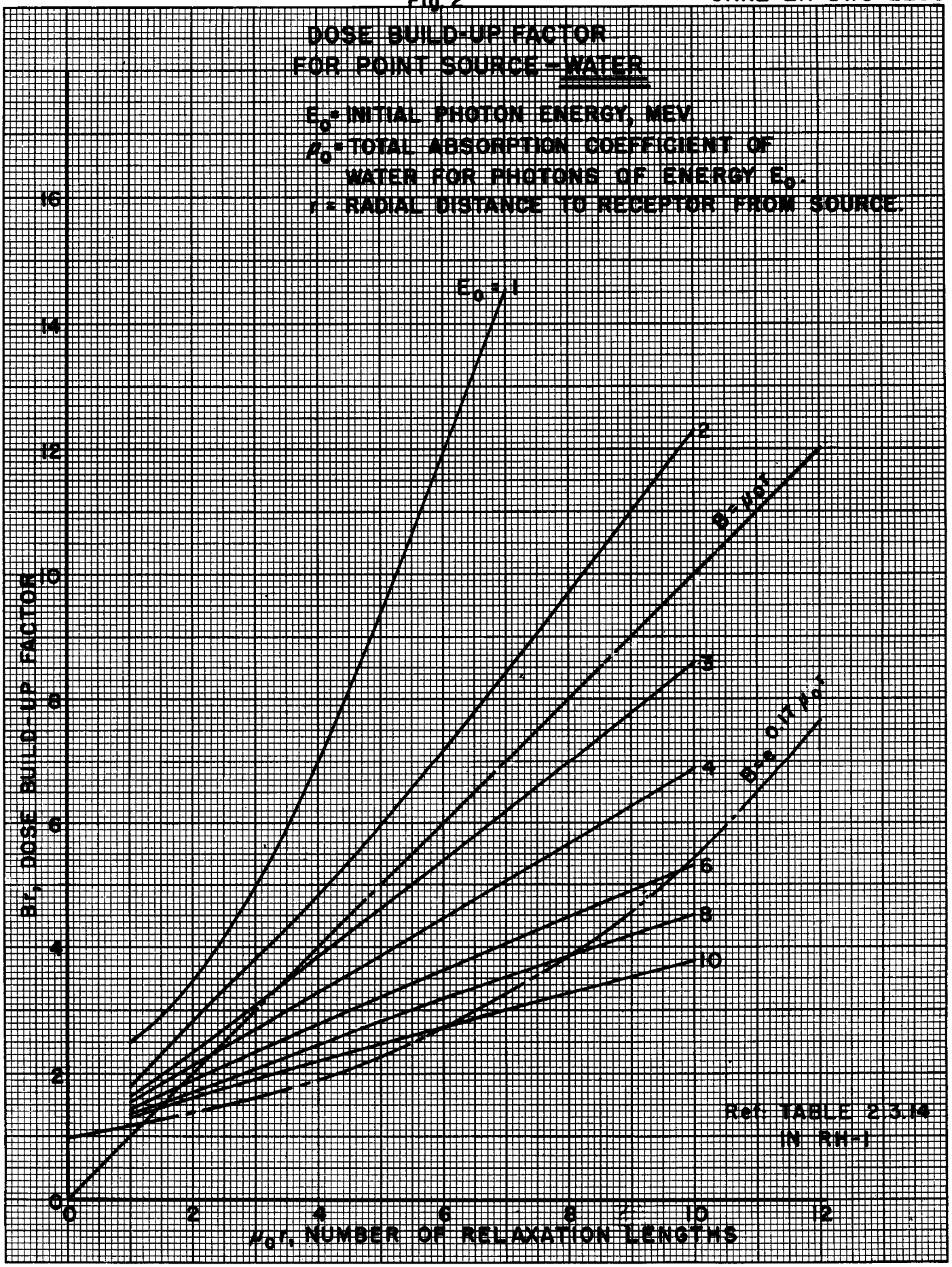

UNCLASSIFIED

ORNL-LR-DWG-2269

Fig. 3

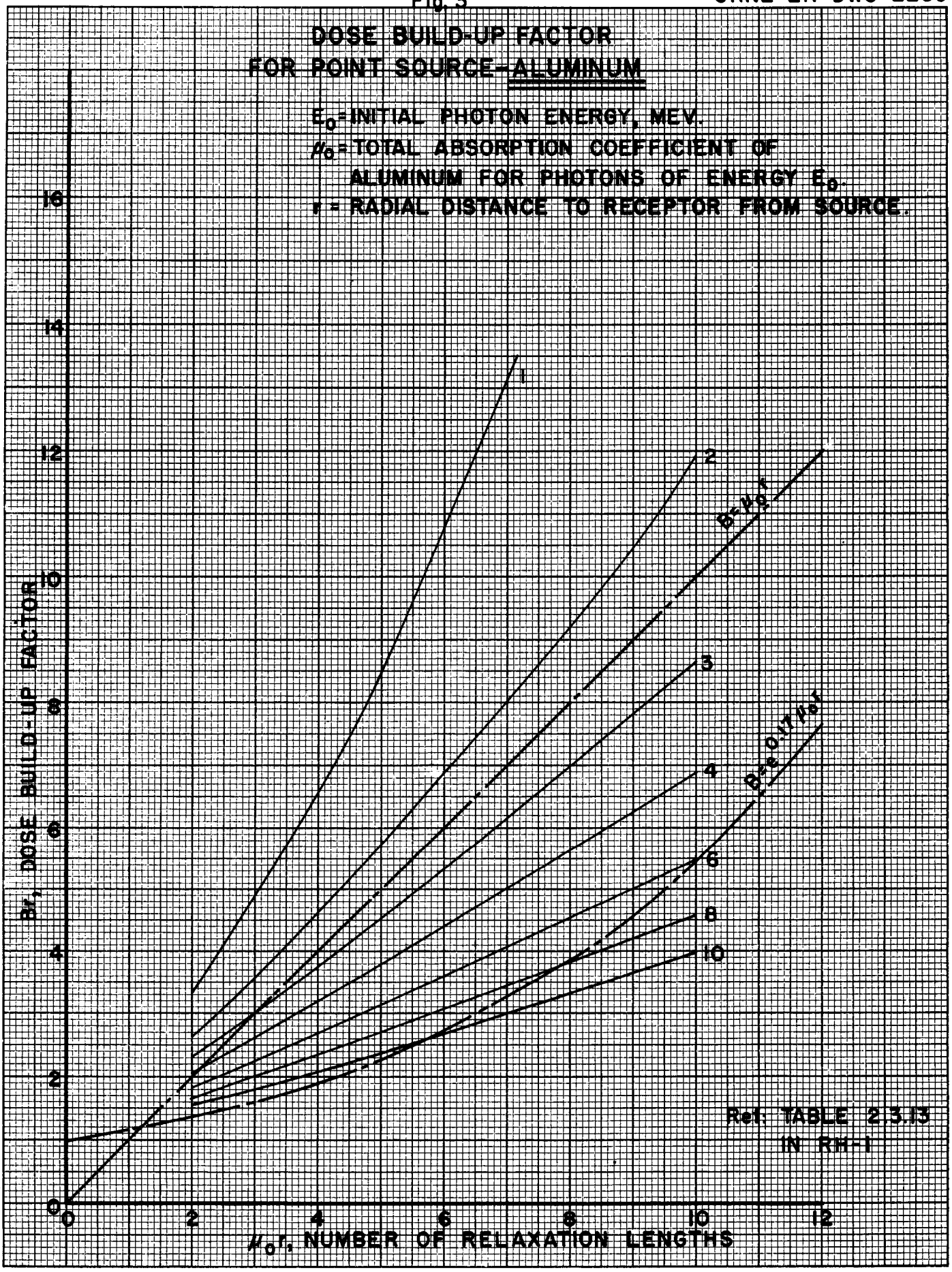

UNCLASSIFIED

Fig. 4

ORNL-LR-DWG-2270

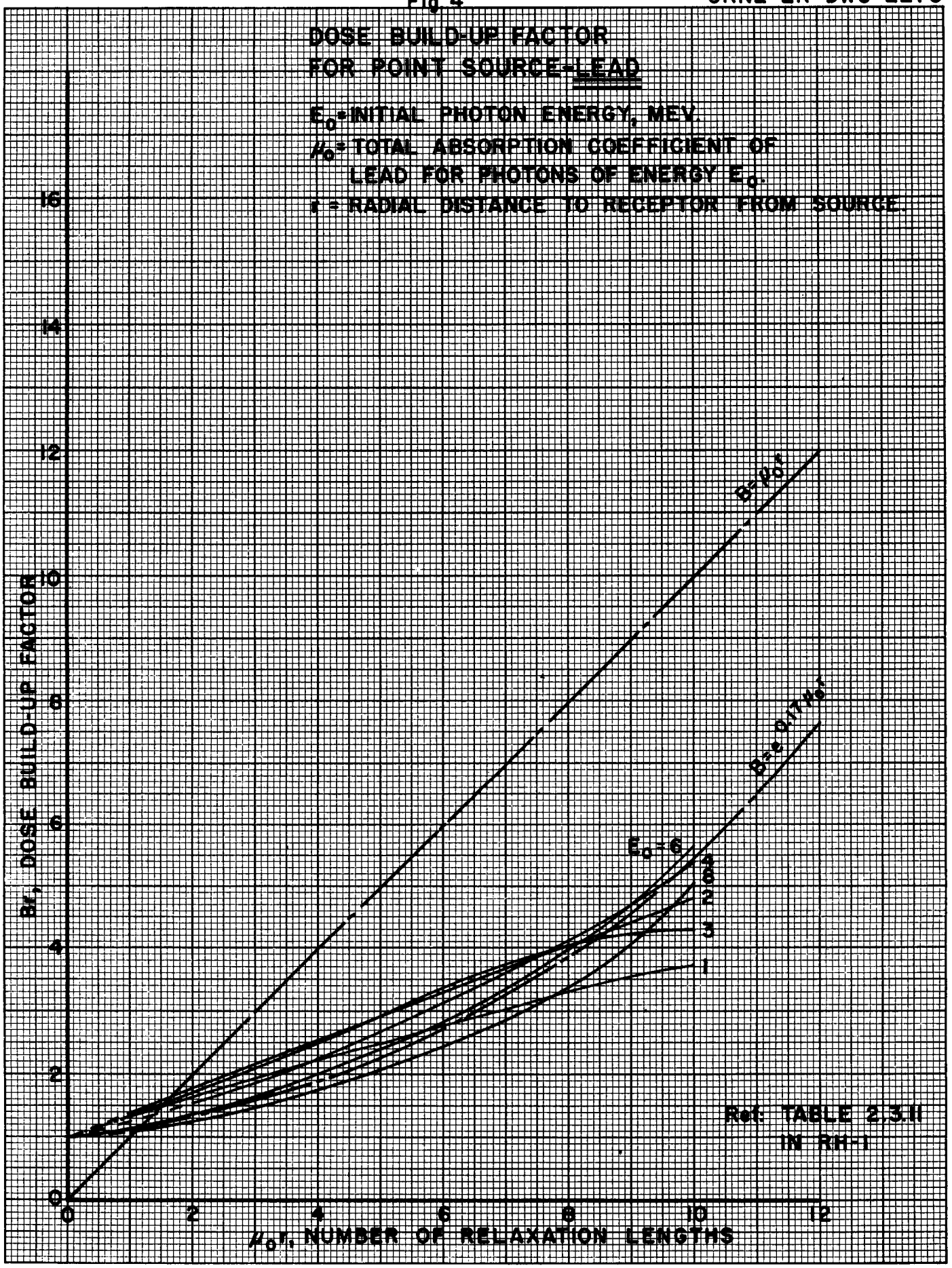

UNCLASSIFIED

ORNL-LR-DWG-3316

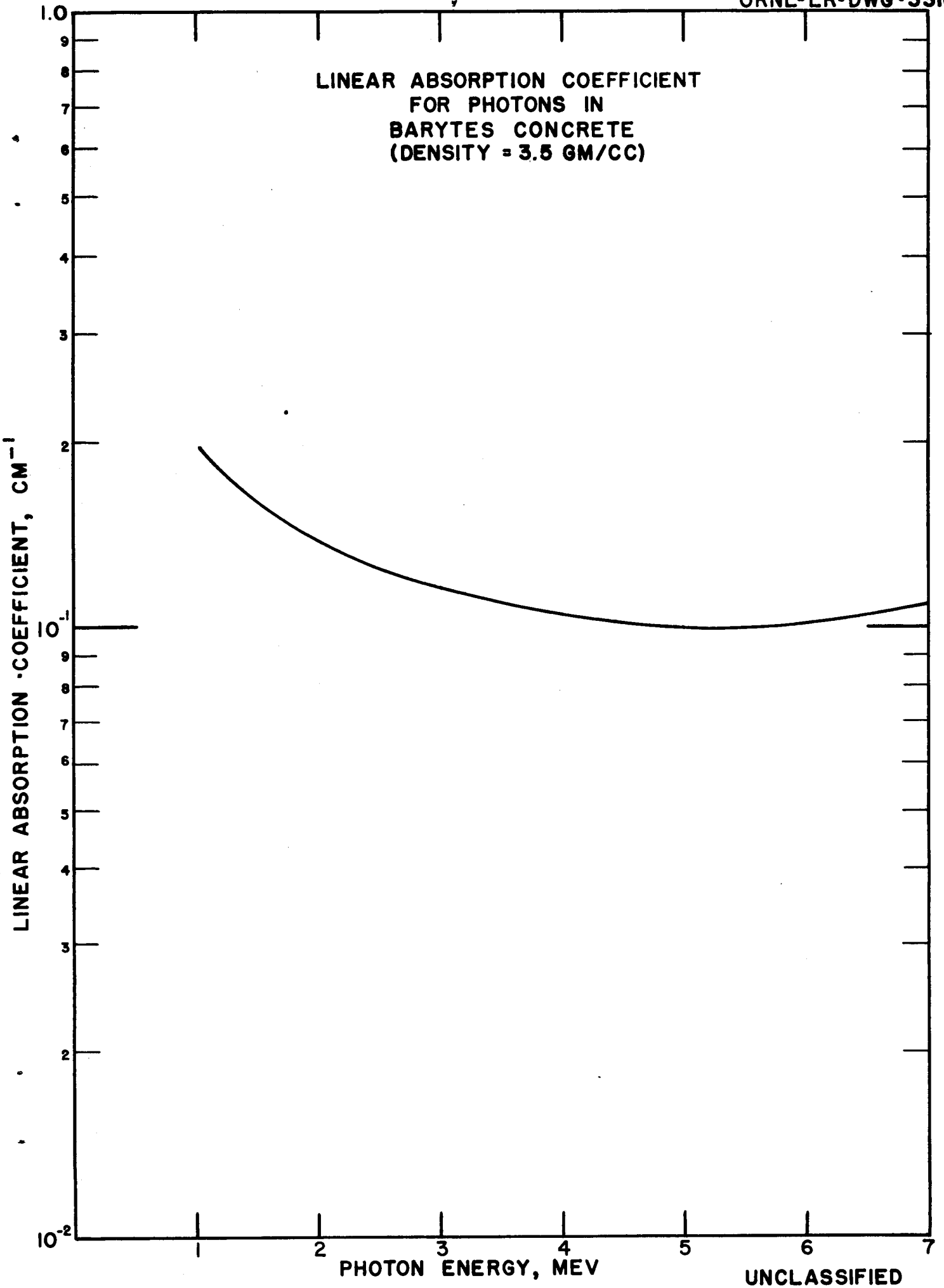

UNCLASSIFIED

ORNL-LR-DWG-3317

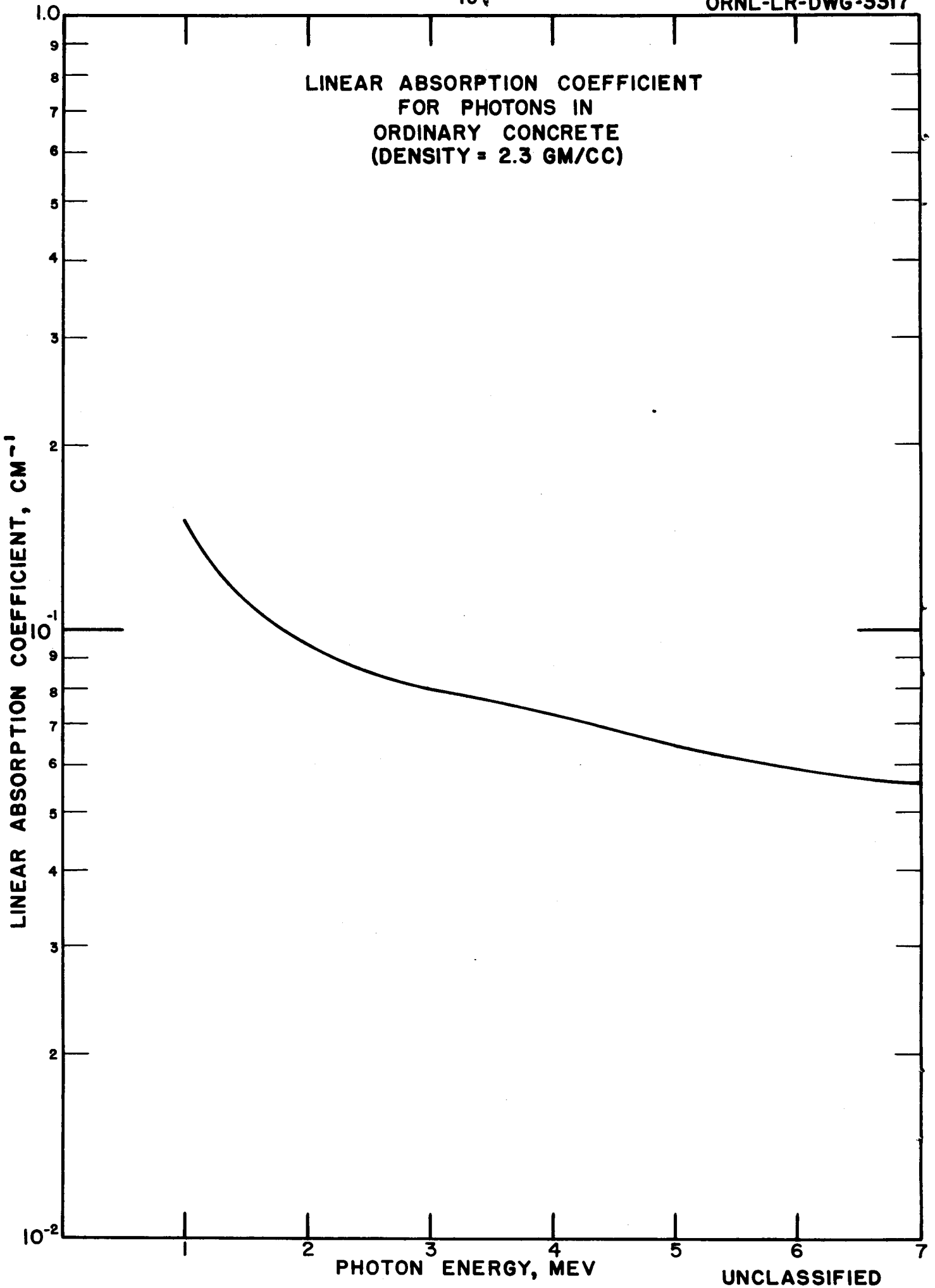

UNCLASSIFIED

APPENDIX c

ACTIVITY PRESENT IN THE COOLING SYSTEM OF THE ORR

F. T. Binford

1. POWER DEPENDENCE OF THE ACTIVITY

Consider a system, operating at a constant pumping rate, which consists of a reactor core, a cooling loop, and a demineralizer through which a fraction η of the coolant flow is diverted. Let C_1 be the concentration of activity (disintegrations per unit time per unit volume) in the effluent from the reactor of some radioisotope, say x. Then if the demineralizer is such that the ratio of activity concentration emerging from it to the activity concentration entering is a constant, say $0 \leq f \leq 1$, neglecting decay, the concentration of activity in the demineralizer effluent, denoted by C_2, will be

$$C_2 = fC_1 \tag{1}$$

The stream leaving the demineralizer then rejoins the main circuit containing the fraction $(1 - \eta)$ which did not pass through the demineralizer. The concentration in this mixed stream, again neglecting decay, will be

$$C_3 = \eta C_2 + (1 - \eta)\, C_1 = C_1 \left\{ 1 - \eta (1 - f) \right\} \tag{2}$$

Since there is decay, due to the time t required for the coolant to traverse the circuit, the activity concentration reentering the reactor will be

$$C_4 = C_1 \left\{ 1 - \eta (1 - f) \right\} e^{-\lambda t} \tag{3}$$

where here λ is the decay constant of x, and the assumption has been made that the circuit time t for coolant passing through the demineralizer is the same as that for coolant not passing through it.

APPENDIX c

If at any given power level, P, the pumping rate is constant and proportional to P, then the increment of concentration gained by the coolant in passing through the reactor will be independent of the power level, provided that the residence time in the core is short compared to the half life of x. Letting this increment be denoted by G we have that at equilibrium

$$C_1 = C_4 + G \tag{4}$$

Thus using equation (3) we obtain

$$C_1 = \frac{G}{1 - \left(1 - \eta(1 - f)\right)e^{-\lambda t}} \tag{5}$$

Where G is determined by the configuration of the system and is the same for systems having identical flux distributions, core sizes, and relations of power to pumping rates.

We distinguish two cases:

(1) The half life of the activity is short compared to the circuit time; in this case equation (5) reduces to

$$C_1 \cong G \tag{6}$$

Thus for a given system the concentration of activity leaving the core is independent of power level provided (a) the residence time in the core is short compared to the half life and (b) the circuit time is long compared to the half life.

(2) The half life of the activity is long compared to the circuit time; in this case equation (5) becomes approximately

$$C_1 \cong \frac{G}{\eta + \lambda t} \tag{7}$$

where here, since η, f, and λt are small we have dropped their products.

APPENDIX c

Since we have taken the pumping rate proportional to the power level, the circuit time t is inversely proportional to the power level. Thus we can write

$$t = K/P \tag{8}$$

where K depends upon the configuration of the system. Putting this into equation (7) we obtain

$$C_1 = \frac{GP}{P\eta + \lambda K} \tag{9}$$

For the special case where η is very small so that $P\eta \ll \lambda K$ we have

$$C_1 = \frac{G}{\lambda K} P \tag{10}$$

This situation obtains when (a) the residence time in the reactor is short compared to the half life and (b) the circuit time is also short compared to the half life.

2. EFFECT OF DEMINERALIZATION

If η is set equal to zero in equation (5) we obtain for the concentration in the case of no demineralization

$$C_1^o = \frac{G}{1 - e^{-\lambda t}} \tag{11}$$

Forming the ratio C_1/C_1^o and utilizing the fact that $f \cong 0$ we have

$$E \equiv C_1/C_1^o = \left(1 + \frac{\eta e^{-\lambda t}}{1 - e^{-\lambda t}}\right)^{-1} \tag{12}$$

For relatively long lived material this becomes

$$E = \frac{\lambda t}{\lambda t + \eta(1 - \lambda t)} \cong \left(1 + \frac{\eta}{\lambda t}\right)^{-1} \tag{13}$$

which gives a measure of the effectiveness of the demineralizer in removing activity

ORNL-LR-DWG-3318

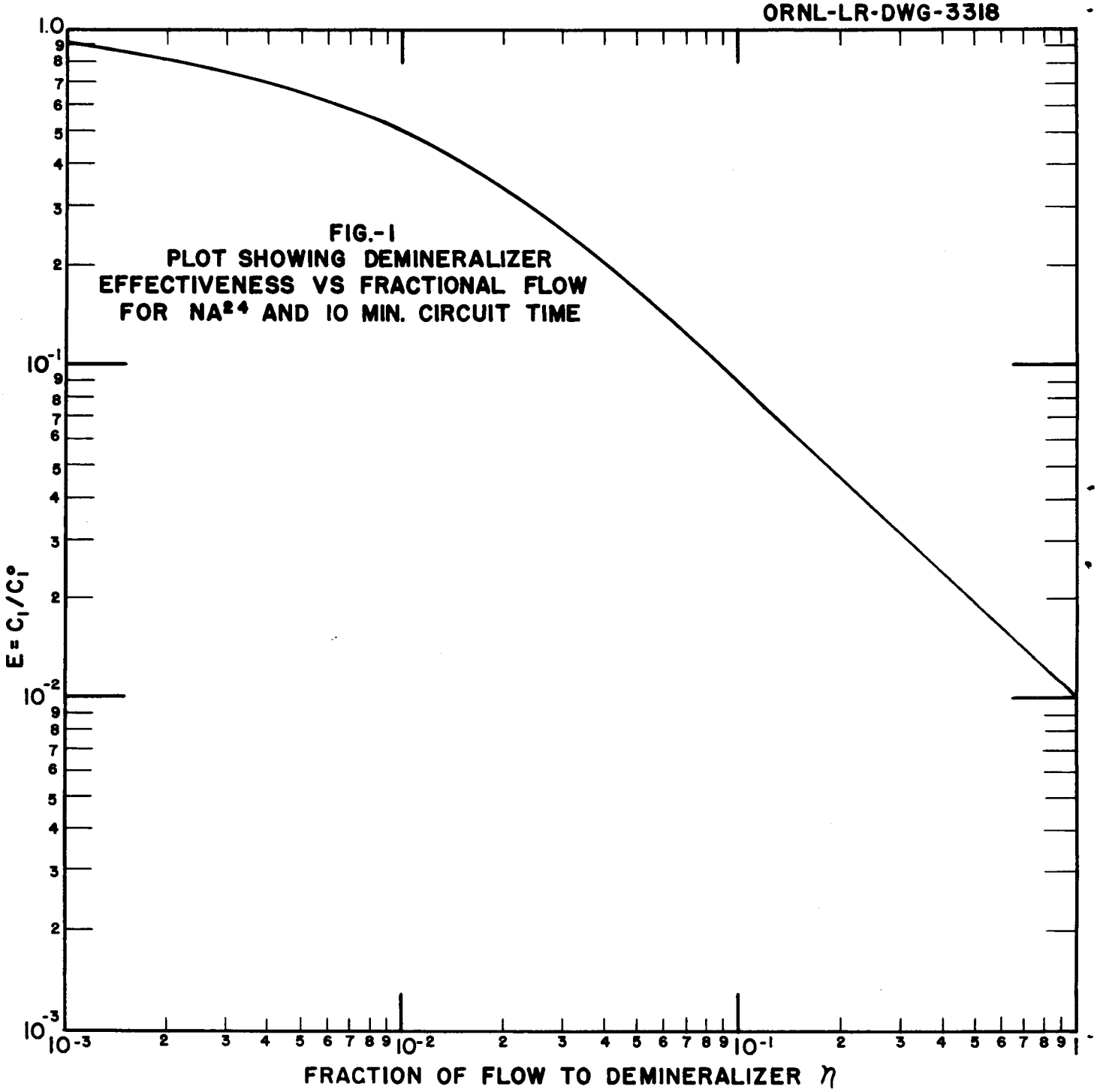

FIG.-1
PLOT SHOWING DEMINERALIZER EFFECTIVENESS VS FRACTIONAL FLOW FOR NA^{24} AND 10 MIN. CIRCUIT TIME

UNCLASSIFIED

APPENDIX c

A graph illustrating this relation for the case of Na^{24} and a 10 minute circuit time is given in figure 1.

3. ESTIMATE OF THE ACTIVITY BASED ON LITR ANALYSIS

A radiochemical analysis of the cooling water leaving the active portion of the LITR core has been made by Lyon and Cox[1]. . Using these results and assuming a cosine distribution of flux across the LITR the following values are obtained for the activity of water leaving the ORR core

Nuclide	Half Life	Gamma Energy	ORR Activity
N^{16}	7.3 sec	7 mev	1.63×10^3 mc/ft^3
Na^{24}	14.9 hr	2.76, 1.38 mev	0.36 mc/ft^3 megawatt
Mg^{27}	9.6 m	0.84, 1.0 (20%)mev	0.50 mc/ft^3 megawatt
Al^{28}	2.3 m	1.80	1.63 mc/ft^3 megawatt

The assumptions used in making the above estimates include direct dependence of activity on power level for the longer lived components, similar pumping and shape characteristics for the LITR and the ORR, and similar demineralization characteristics. The estimates are somewhat conservative.

(1) ORNL CF-54-9-99

APPENDIX d

ESTIMATE OF THE SHIELDING REQUIRED FOR PIPELINES CARRYING N^{16}-BEARING WATER

F. T. Binford

The amount of concrete shielding required to reduce the radiation, from pipe lines of various sizes, bearing N^{16} in solution, to approximately 0.75 mr/hr has been computed using the method of the equivalent line source(1). The absorption coefficients, which include a 17% correction in the exponential for buildup, were 0.06 in^{-1} for water and 0.12 in^{-1} for concrete. The results are given graphically in the attached figure.

Similar calculations for the residual Na^{24}, Mg^{27}, and Al^{28} activity assuming complete decay of N^{16} and concentrations of the remaining radioisotope as given in appendix c yield the following results:

Pipe Size	Concrete to Reduce to 1 mr/hr at 10 mw
6"	12"
12"	18"
18"	18"

(1) PROJECT HANDBOOK V

ORNL-LR-DWG-3319

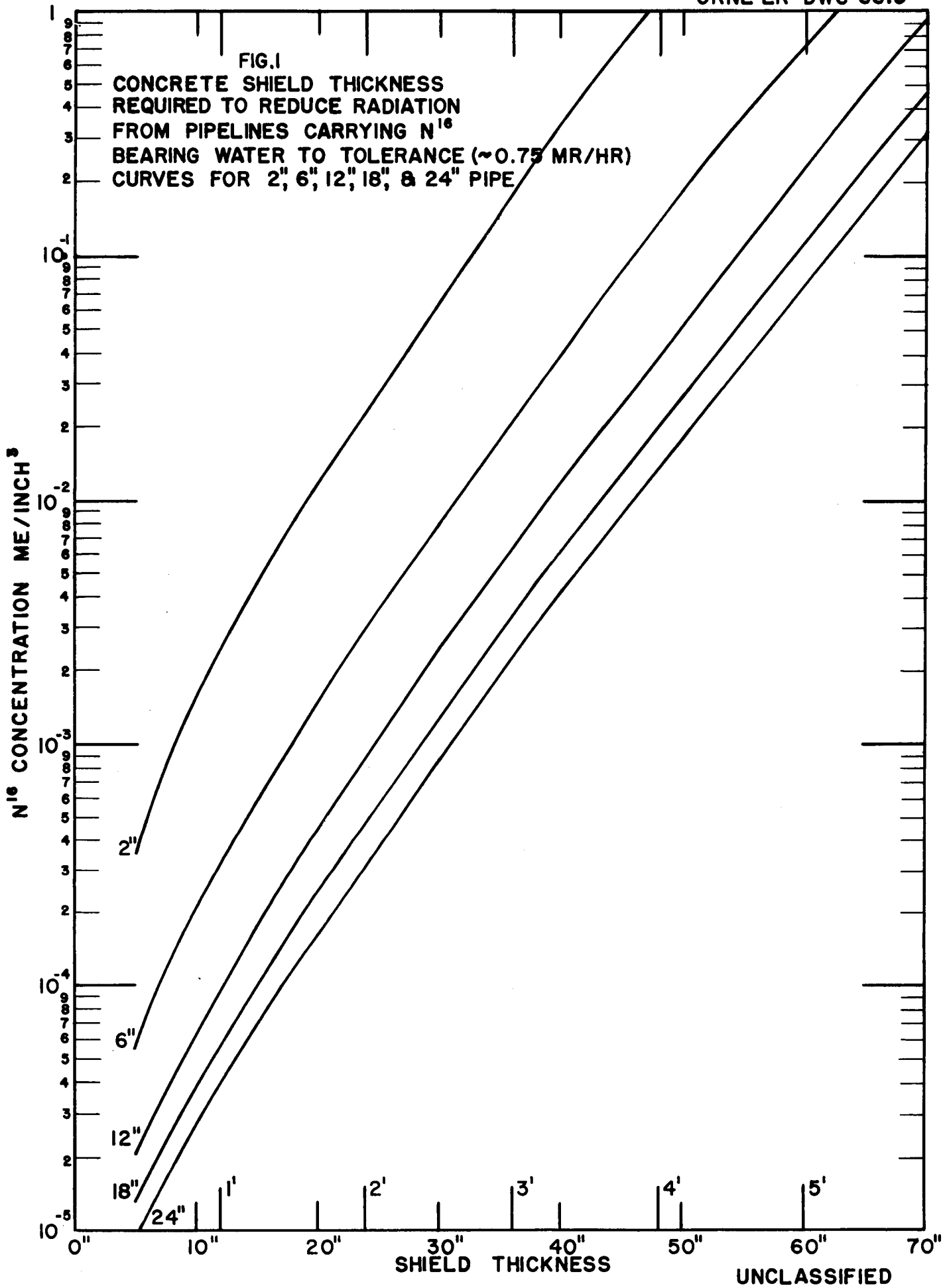

UNCLASSIFIED

APPENDIX e

AN ESTIMATE OF THE AMOUNT OF BARYTES CONCRETE REQUIRED TO SHIELD THE CEILING OF THE ORR PUMP CUBICLES

F. T. Binford

Since the cooling water from the reactor core may still contain appreciable quantities of N^{16} when it enters the pump cubicle it is necessary to determine the amount of shielding necessary to afford protection from the resultant gamma flux.

The source strength present in water leaving the reactor has been determined (1) to be approximately 1.63 curies of N^{16} per cubic foot. Based on design flow rates at various power levels the source strength in water entering the cubicle is computed to be:

Power Level (mw)	Source (Photons/ft^3 sec)
5	3×10^6
10	4.1×10^8
30	1.2×10^{10}

For the purpose of this estimate the pump cubicle is consdered to contain an infinite straight length of 12" pipe which lies in the horizontal plane and a vertical 18" diameter 4' high pipe intersecting it. Both of these contain uniformly distributed sources of 7 mev gamma rays as indicated above.

Using the method of Taylor and Obenshain[2] for the case of the infinitly long pipe, and a numerical method involving disk sources for the vertical pipe, the radiation intensity in terms of a tolerance level of 10^5 photons/ft^2 sec[3] is given on the next page. Here the point of observation is taken as 8.2' from the center line of the 12" pipe.

APPENDIX e

Shield Thickness (ft) Barytes Concrete	Fraction of Tolerance (0.75 mr/hr)		
	5 mw	10 mw	30 mw
0	11.7	1600	46,900
0.36	2.7	366	10,700
1.07	.22	29.8	871
1.80	2.3×10^{-2}	3.2	93.8
3.57	10^{-4}	1.4×10^{-2}	.415
5.31	5×10^{-7}	7×10^{-5}	2×10^{-3}

These results are presented graphically in figure (1).

At 5 mw operation the radiation intensity in the cubicle near the pipeline will be of the order of 500 mr/hour and at 10 mw of the order of 1000 mr/hour.

The absorption coefficients used in these calculations are[3]

for 7 mev γ rays in H_2O 0.61 ft^{-1}

for 7 mev γ rays in Barytes 2.81 ft^{-1}

References

(1) Letter, F. T. Binford to ORR File, 7/13/54

(2) WAPD-RM-213

(3) CF-54-7-95, N. F. Lansing

Fig. 1

ORNL-LR-DWG. 3058

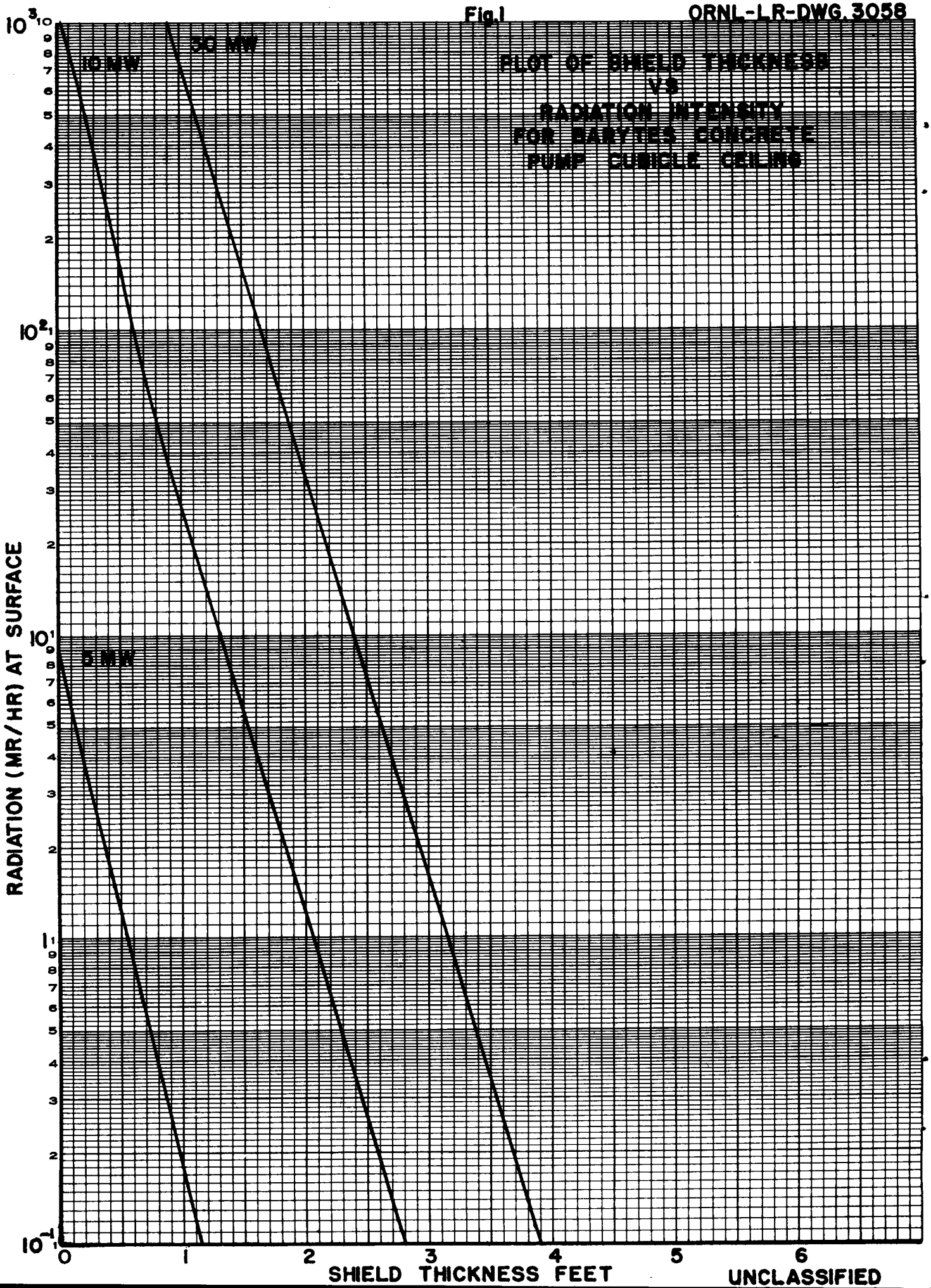

UNCLASSIFIED

APPENDIX f

ESTIMATE OF THE RADIATION INTENSITY AT THE ORR COOLING LOOP HEAT EXCHANGERS

F. T. Binford

The tubes of the cooling loop heat exchanger lie in a horizontal plane approximately 55' long and 30' wide. These tubes contain a total of approximately 100 gallons of water.

The radiation intensity in the vicinity of the heat exchanger is estimated by considering it to be a uniform disk source, having the same area as the rectangular tube bed, and computing the intensity along the axis of this disk.

The source terms used are those given in appendix c. Since approximately 2 minutes are required for cooling water to come from the reactor at 5 mw operation and 75 seconds are required at 10 mw operation; the appropriate decay factors have been introduced.

The calculation yields the following intensities at a point on the axis of the disk 5' from the surface:

Power Level	Radiation Intensity
5 mw	16 mr/hr
10 mw	29 mr/hr

APPENDIX g

AN ESTIMATE OF THE CONTRIBUTION TO THE RADIATION INTENSITY ABOVE THE SURFACE OF THE RESEARCH REACTOR DUE TO THE PRESENCE OF NITROGEN 16

F. T. Binford

For the purpose of this estimate the reactor is idealized to consist of two coaxial cylinders and a sphere as shown in Figure 1. The dimensions of the system are indicated on this diagram. The outer cylinder represents the pool; the inner cylinder the core tank; and the sphere the reactor core. Both pool and core tank are filled with water, but it is assumed there is no connection between them, and hence no interchange of water between the two.

During operation of the reactor, nitrogen 16 is formed by the O^{16} (η,ρ) N^{16} reaction [1] and this activity is conveyed upward by convection currents which are set up due to uneven heating in the system.

I. ESTIMATE OF THE OVERALL N^{16} PRODUCTION

On making this estimate the following assumptions are used:

(i) Since the O^{16} (η,ρ) N^{16} reaction has a threshold of 12.2 mev [1] we will assume that N^{16} atoms are produced only by the action of the uncollided flux above this threshold. This is equivalent to the assumption that no neutrons which have suffered at least one collision remain above 12.2 mev in energy (Rough calculations indicate that this is true for about 90% of the cases in question)

(ii) The energy spectrum of neutrons leaking from the core is sensibly the same as the fission spectrum.

(iii) The dimensions of the cylindrical pool are large compared to the mean free path of the uncollided neutrons so that the fraction of uncollided flux reaching the pool walls is sensibly zero.

Let us denote by $\mathcal{L}$ the number of neutrons, capable of producing the $O^{16}(\eta,\rho)$ N^{16} reaction, which leak from the core per second.

APPENDIX g

Under the assumptions stated above these neutrons will either enter the N^{16} reaction or will be scattered out of competition. Let the average cross sections for these processes be Σ_a and Σ_s respectively. Then the fraction of available neutrons which participate in the $O^{16}(n,p)N^{16}$ reaction may be written as

$$\Sigma_a / (\Sigma_a + \Sigma_s) = \beta \tag{1}$$

The total rate of production of N^{16} atoms, denoted by $\mathcal{P}_a$, can then be written as

$$\mathcal{L}\beta = \mathcal{P}_a \text{ atoms/second} \tag{2}$$

For convenience we convert this to curies per second by multiplying through by λ, the decay constant in seconds^{-1} of N^{16} and dividing by the numerical factor $c = 3.7 \times 10^{10}$ curies^{-1}. Thus if we let $\mathcal{P}_c$ be the production rate in curies per second we have

$$\frac{\mathcal{L}\beta\lambda}{c} = \mathcal{P}_c \text{ curies/second} \tag{3}$$

II ESTIMATE OF THE SPATIAL DISTRIBUTION OF THE PRODUCTION RATE

We here introduce the assumption that the uncollided flux from the core falls off as $\varphi^{-2} e^{-\mu\varphi}$ where μ is the e-folding length for the neutrons under consideration and φ is the distance from the center of the spherical reactor. Then the production per unit volume at space point φ is proportional to the flux at that point, and we have, denoting the production per unit volume by $\xi(\varphi)$, the relation

$$\xi(\varphi) = \frac{\mathcal{N} e^{-\mu\varphi}}{\varphi^2} \text{ curies/unit volume.second} \tag{4}$$

where $\mathcal{N}$ is a constant.

APPENDIX g

The constant $\mathcal{K}$ can be determined by the requirement that

$$P_c = \mathcal{K} \int_{\text{VOLUME OF POOL}} \frac{e^{-\mu\varphi}}{\varphi^2} dV \tag{5}$$

Since we have assumed essentially no production at distances greater than $\varphi = R_0$ from the core center, it will be a reasonable procedure to perform this integration over the region lying between the core of radius R_2 and a sphere of radius R_0. Thus

$$P_c = 4\pi\mathcal{K} \int_{R_2}^{R_0} \frac{e^{-\mu\varphi}}{\varphi^2} \cdot \varphi^2 d\varphi = \frac{4\pi\mathcal{K}}{\mu}\left[e^{-\mu R_2} - e^{-\mu R_0}\right] \tag{6}$$

Since the second factor on the right hand side is small compared to the first we can neglect it and write approximately

$$\mathcal{K} = \frac{\mu P_c e^{\mu R_2}}{4\pi} \tag{7}$$

Hence

$$\xi(\varphi) = \frac{\mu P_c e^{\mu R_2}}{4\pi} \cdot \frac{e^{-\mu\varphi}}{\varphi^2} \quad \text{curies/unit volume sec} \tag{8}$$

III THE SPATIAL DISTRIBUTION OF ACTIVITY

We now wish to examine the vertical distribution of activity due to the presence of both production and convection. N. F. Lansing [2] has shown that in the configuration under consideration, upward flow originates in three main areas as illustrated in Figure (2). There is an annular region of flow about the core tank, a cylindrical column of flow above the tank and two thin rectangular sheets of flow above the water inlet lines to the core tank.

APPENDIX g

Due to the dimensions of the system under consideration the contribution to the total activity originating in these last two regions is very small compared to the activity which originates in the annular region about the core tank. Accordingly we will neglect these in the following treatment. The assumptions employed are

(i) The thickness of the annular region (1), t, is small compared to the radius R_1 of the core tank.

(ii) The upward flow takes place at a constant velocity v.

(iii) For the purpose of computation we will initially suppose that the upward flow does not spread out laterally, but behaves as if it were confined to the region between two concentric cylinders of radii R_1 and $R_1 + t$ respectively.

The geometric configuration is illustrated in Figure (3). Since t, the thickness of the annulus is small compared to the radius R_1 we can write for the production per unit volume in a region located a distance z above the plane of the reactor

$$\xi(z) = \frac{\gamma e^{-\mu\sqrt{z^2+R_1^2}}}{z^2+R_1^2} \tag{9}$$

We now let $\eta(z)$ be the concentration in curies per unit volume at z and write the balance equation

$$2\pi R_1 t v \eta(z) + 2\pi R_1 t\, dz\, \xi(z) - 2\pi R_1 t v \eta(z+dz) - 2\pi R_1 t\, dz\, \lambda \eta(z) = 0 \tag{10}$$

or

$$\frac{d\eta(z)}{dz} + \frac{\lambda}{v}\eta(z) = \frac{1}{v}\xi(z) \tag{11}$$

Where λ is the decay constant of N^{16}.

As a boundary condition we require that

$$\eta(-\infty) = 0 \tag{12}$$

APPENDIX g

Whence we obtain for the concentration at z

$$\eta(z) = \frac{1}{v} e^{-\lambda z} \int_{-\infty}^{z} e^{\lambda u/v} \xi(u)\, du \tag{13}$$

which upon introducing equation (9) becomes

$$\eta(z) = \frac{\mathcal{H}}{v} e^{-\lambda z/v} \int_{-\infty}^{z} \frac{e^{-\mu\sqrt{u^2+R_1^2} + \lambda u/v}}{u^2+R_1^2}\, du \tag{14}$$

Now in the cases under consideration $\mu \gg \lambda/v$ and since we will be interested in rather large values of z the integral in equation (14) can be approximated as

$$\int_{-\infty}^{z} \frac{e^{-\mu\sqrt{u^2+R_1^2} + \lambda u/v}}{u^2+R_1^2}\, du \cong \int_{-\infty}^{\infty} \frac{e^{-\mu\sqrt{u^2+R_1^2} + \lambda u/v}}{u^2+R_1^2}\, du \equiv I \tag{15}$$

where I is independent of z. Thus

$$\eta(z) = \frac{\mathcal{H} I}{v} e^{-\lambda z/v} \quad \text{curies/unit volume} \tag{16}$$

So far the upward flow has been considered as if it continued indefinitely in the positive z direction. Actually the flow spreads out as it rises and then sinks along the cooler outer walls of the pool. To describe the situation we will consider that the upward flow continues until it reaches the surface of the pool where it spreads out radially and then sinks slowly along the pool circumference as illustrted in Figure (4). Thus we have three regions of activity all of which are considered to be far enough above the core itself so that there is virtually no direct contribution to the activity due to production.

APPENDIX g

(i) An annular region of radius R_1 and wall thickness t rising through the center of the pool.

(ii) A doughnut-shaped region of inner radius R_1, outer radius R_0 and thickness S which lies on the surface of the pool. Here the flow is radial; outward from the center.

(iii) An annular region of radius R_0 and wall thickness t' in which the liquid is falling along the sides of the cylindrical pool.

We consider now the first region. The concentration per unit volume at height z is given by equation (16). Thus the total activity in an annulus of radius R_1 thickness t and height unity is

$$\phi_1(z) = \frac{2\pi R_1 t \mathcal{H} I}{v} e^{-\lambda z/v} \qquad \text{curies/unit height} \qquad (17)$$

For the third region we must, if the velocity is to be preserved, have the same cross sectional area. Thus

$$t' = R_1 t / R_0 \qquad (18)$$

and since the flow must have reached and crossed the top of the pool

$$\phi_3(z) = \frac{2\pi R_0 t' \mathcal{H} I}{v} e^{-\lambda(2H_0 + R_0 - R_1 - z)/v}$$

or

$$\phi_3(z) = \frac{2\pi R_1 t \mathcal{H} I}{v} e^{-\lambda(2H_0 + R_0 - R_1)} \cdot e^{\lambda z/v} \qquad \text{curies/unit height} \qquad (19)$$

We examine now the doughnut shaped section on the pool surface. We denote by S the thickness of this region. Thus

$$S = 2R_1 t / (R_0 + R_1) \qquad (20)$$

The total activity per unit radius in an annular region of thickness S lying on the surface at a radial distance r from the center is

$$\phi_2'(r) = \frac{2\pi R_1 t \mathcal{H}}{v} I e^{-\lambda(H_0 + r - R_1)/v}$$

APPENDIX g

or, upon spreading the activity out over the area of the disk

$$\phi_2(r) = \frac{R_1 t \mathcal{H} I}{r v} e^{-\lambda(H_0 - R_1)/v} \cdot e^{-\lambda r/v} \qquad \text{curies/unit area} \quad (21)$$

$$R_1 \leq r \leq R_0$$

Summarizing then we have

REGION 1. Rising column in center of radius R_1 and wall thickness t

$$\phi_1(z) = G e^{-\lambda z/v} \qquad \text{curies/unit height} \quad (22)$$

REGION 2. Doughnut shaped region on the surface, having inner radius R_1 and outer radius R_0 and thickness S

$$\phi_2(r) = \frac{G}{2\pi r} e^{-\lambda(H_0 - R_1)/v} \cdot e^{-\lambda r/v} \qquad \text{curies/unit area} \quad (23)$$

REGION 3. Falling column at pool circumference, having radius R_0 and wall thickness t'

$$\phi_3(z) = G e^{-\lambda(2H_0 + R_0 - R_1)/v} \cdot e^{\lambda z/v} \qquad \text{curies/unit height} \quad (24)$$

where the quantity G is defined as

$$G \equiv \frac{2\pi R_1 t \mathcal{H} I}{v} = \frac{R_1 t \mu \mathcal{L} \Sigma_a \lambda e^{\mu R_2}}{2 v c (\Sigma_a + \Sigma_s)} \int_{-\infty}^{\infty} \frac{e^{-\mu\sqrt{u^2 + R_1^2} + \lambda u/v}}{u^2 + R_1^2} \, du \qquad (25)$$

IV RADIATION INTENSITY ON THE EXTENDED AXIS OF THE POOL

We consider first the contribution from the doughnut shaped region 2 at a point on the pool axis a distance h above the pool surface. We will assume here a flat source distribution and no attenuation due to the water.

APPENDIX g

Then the intensity at a point on the axis a distance H_0+h from the center of the reactor due to this region is

$$I_2(h) = K\int_0^{2\pi}\int_{R_1}^{R_0} \frac{\phi_2(r)\, r\,dr\,d\theta}{r^2+h^2} \tag{26}$$

where here K is a constant relating activity in curies at a point to intensity in roentgens/hour at unit distance from the point. Thus

$$I_2(h) = KG\,e^{-\lambda(H_0-R_1)/v}\int_{R_1}^{R_0} \frac{e^{-\lambda r/v}}{r^2+h^2}\,dr \tag{27}$$

This integral can easily be evaluated by using the approximation

$$e^{-x} \cong 1 - x + x^2/2$$

where x is a small positive number. Thus

$$I_2(h) = KG\,e^{-\lambda(H_0-R_1)/v}\left\{\left(\frac{1}{h} - \frac{\lambda^2 h}{2v^2}\right)\left(\tan^{-1}\frac{R_0}{h} - \tan^{-1}\frac{R_1}{h}\right) + \frac{\lambda^2}{2v^2}(R_0-R_1) - \frac{\lambda}{2v}\ln\left(\frac{R_0^2+h^2}{R_1^2+h^2}\right)\right\} \tag{28}$$

We consider now the contributions from the annular regions as illustrated in Figure (5). In both cases we can write a differential equation of the form

$$dI = \frac{K\phi(z)\,B(\gamma l)\,e^{-\gamma l}}{(H_0+h-z)^2+R^2}\,dz \tag{29}$$

Where γ is the absorption coefficient in water for gamma rays of the energy under consideration, l is the distance in water between a point on the elemental ring of activity and the point of observation P, and $B(\gamma l)$ is the buildup factor. From the geometry of the system we see that

$$l = \frac{H_0-z}{H_0+h-z}\sqrt{(H_0+h-z)^2+R^2} \tag{30}$$

APPENDIX g

in particular we have for region 1

$$dI_1(h) = KG \frac{B(\gamma l_1) e^{-\gamma l_1 - \lambda z/v}}{(\mathcal{H}_0 + h - z)^2 + R_1^2} dz \tag{31}$$

$$l_1 = \frac{\mathcal{H}_0 - z}{\mathcal{H}_0 + h - z} \sqrt{(\mathcal{H}_0 + h - z)^2 + R_1^2} \tag{32}$$

and for region 3

$$dI_3(h) = KG \frac{e^{-\lambda(2H_0 + R_0 - R_1)/v} B(\gamma l_3) e^{-\gamma l_3 + \lambda z/v}}{(\mathcal{H}_0 + h - z)^2 + R_0^2} \tag{33}$$

$$l_3 = \frac{\mathcal{H}_0 - z}{\mathcal{H}_0 + h - z} \sqrt{(\mathcal{H}_0 + h - z)^2 + R_0^2} \tag{34}$$

Equations (31) and (33) are to be integrated between $\mathcal{H}_0 - S$ and some value of z, say z_0, below which the contribution to the intensity is negligible. Thus the intensity at P is

$$I(h) = KG \left\{ e^{-\lambda(H_0 - R_1)/v} \left[\left(\frac{1}{h} - \frac{\lambda^2 h}{2v^2}\right)\left(\tan^{-1}\frac{R_0}{h} - \tan^{-1}\frac{R_1}{h}\right) + \frac{\lambda^2}{2v^2}(R_0 - R_1) - \frac{\lambda}{2v} \ln\left(\frac{R_0^2 + h^2}{R_1^2 + h^2}\right) \right] + \int_{z_0}^{\mathcal{H}_0 - S} \frac{B(\gamma l_1) e^{-\gamma l_1 - \lambda z/v}}{(\mathcal{H}_0 + h - z)^2 + R_1^2} dz + e^{-\lambda(2H_0 + R_0 - R_1)/v} \int_{z_0}^{\mathcal{H}_0 - S} \frac{B(\gamma l_3) e^{-\gamma l_3 + \lambda z/v}}{(\mathcal{H}_0 + h - z)^2 + R_0^2} dz \right\} \tag{35}$$

V EVALUATION OF THE CONSTANTS

We first consider the quantity $\mathcal{L}$ which is defined to be the number of neutrons, having energies sufficiently high to enter the $O^{16}(n,p)N^{16}$, reaction which leak from the reactor core per unit time. This could be estimated using the value of $(K_\infty - 1)/K_\infty$ for this type of reactor. A more conservative figure is obtained by using the power density and the relaxation length of the high energy neutrons in the reactor. We will assume this to be the same in the reactor as in water i.e., $(\Sigma_a + \Sigma_s)^{-1}$

APPENDIX g

Then if W is the power density in watts per unit volume, A is the surface area of the core, α is the number of fissions per second per watt, ν is the number of neutrons appearing per fission, and f is the fraction of these above 12.2 mev we have

$$\mathcal{L} = \frac{WA\alpha\nu f}{\Sigma_a + \Sigma_s} \qquad \text{high energy neutrons/second} \tag{36}$$

We assume now that Watt's fission spectrum[3] holds in the region under consideration. Thus

$$f = 0.484\int_{12.2}^{\infty} \sinh\sqrt{2E}\, e^{-E}\, dE = 2.5 \times 10^{-4} \tag{37}$$

Thus the total production rate becomes, using equation (3)

$$\frac{WA\alpha\nu f \Sigma_a \lambda}{c(\Sigma_a + \Sigma_s)^2} = P_c \qquad \text{curies/second} \tag{38}$$

Now μ is just $(\Sigma_a + \Sigma_s)$. Therefore we have

$$\mathcal{H} = \frac{WA\alpha\nu f \Sigma_a \lambda e^{(\Sigma_a + \Sigma_s)R_2}}{4\pi c(\Sigma_a + \Sigma_s)} \tag{39}$$

Consider now the integral of equation (15)

$$I = \int_{-\infty}^{\infty} \frac{e^{-\mu\sqrt{u^2 + R_1^2} + \lambda u/v}}{u^2 + R_1^2}\, du \tag{40}$$

This can be written in the form

$$I = 2\int_{0}^{\infty} \frac{e^{-\mu\sqrt{u^2 + R_1^2}} \sinh \lambda u/v}{u^2 + R_1^2}\, du \tag{41}$$

APPENDIX g

Since $\mu \gg \lambda/v$ this can be written approximately as

$$I \cong 2\int_0^\infty \frac{e^{-\mu\sqrt{u^2+R_1^2}}}{v(u^2+R_1^2)}\lambda u\, du = \frac{2\lambda}{v}\int_{\mu R_1}^\infty \frac{e^{-y}}{y}dy = \frac{2\lambda}{v}\left[-Ei(-\mu R_1)\right] \tag{42}$$

Thus using equation (39) and (42) in equation (25) we obtain

$$G = \frac{R_1 \pm \lambda^2}{v^2}\,\frac{WA\alpha\nu f\Sigma_a}{C(\Sigma_a+\Sigma_s)}\left[-Ei\left(-\{\Sigma_a+\Sigma_s\}R_1\right)\right]e^{(\Sigma_a+\Sigma_s)R_2} \tag{43}$$

Now if we assume that Watt's fission spectrum[3] holds in the region in question we have

$$f = 0.484\int_{12.2}^\infty \sinh\sqrt{2E}\; e^{-E}dE = 2.5\times10^{-4} \tag{44}$$

VI NUMERICAL RESULTS

For the system under consideration we have the following constants

R_0 = 5 ft	H_0 = 24 ft	A = 8.04 ft	C = 3.7×10^{10} dis/curie
R_1 = 2.25 ft	H_1 = 8 ft	α = 3.1×10^{10} fissions/sec Watt	ν = 2.5 neuts/fiss
R_2 = 0.8 ft	v = 1 ft/sec	W = 2.802×10^5 Watts/ft^3	f = 2.5×10^{-4}
t = 0.167 ft	λ = 0.0943 sec^{-1}	P = power level megawatts	K = 42 Roentgens/curie

Using these values we obtain

$$G = \frac{3.944\Sigma_a}{\Sigma_a+\Sigma_s}\left[-Ei\left(-2.25\{\Sigma_a+\Sigma_s\}\right)\right]e^{-0.8(\Sigma_a+\Sigma_s)} \tag{45}$$

Since $\Sigma_s \gg \Sigma_a$ it is clear that G varies directly with Σ_a. The variation of G with $\Sigma_a + \Sigma_s$ is shown in Figure 6.

The value of $\Sigma_a + \Sigma_s$ is given by Caswell[4] as

$$\Sigma_a + \Sigma_s = 2.1 \text{ ft}^{-1}$$

APPENDIX g

The value of Σ_a is not well known, but is given by Cochran as[5]

$$\Sigma_a = 0.21 \text{ ft}^{-1}$$

Other authors[6] [7] report smaller values of this cross section, but it is better here to take the more conservative value. Thus

$$G = 3.38 \text{ Px } 10^{-3}$$

We compute $I(h)$ for $h = 1$ foot.

$$I_2(1) = 0.142^{-2.05} (1 - 0.0044)(\tan^{-1}5 - \tan^{-1}2.25) + 0.0044(2.75) - 0.0472 \ln 4.29$$

$$I_2(1) = 0.003\,P \quad \text{Roentgens/hour}$$

The contributions from the annular regions (1) and (3) can be computed numerically. We have

$$\Delta I_1(h) = KG \frac{B(\gamma l_1)\, e^{-\gamma l_1 - \lambda z/v}}{(H_0 + h - z)^2 + R_1^2} \Delta z \tag{46}$$

For a buildup factor we take

$$B(\gamma l) = 1 + 0.23\gamma l \tag{47}$$

and for 7 mev gamma rays[8]

$$\gamma = 0.76 \text{ ft}^{-1}$$

Thus using the value of l_1, given in equation (32) and taking $S = 0.1$ ft we have

$$\Delta I_1(1) = 0.142P \left\{ \frac{1 + 0.17\left[\frac{24-z}{25-z}\sqrt{(25-z)^2 + 5.06}\right]}{(25-z)^2 + 5.06} \right\} e^{-0.76\left[\frac{24-z}{25-z}\sqrt{(25-z)^2+5.06}\right] - .0943z} \Delta z \tag{48}$$

Numerical integration from $z = 20.25$ to $z = 23.9$ yields

$$\Delta I_1\ (1) = 1.44 \times 10^{-3} P \quad \text{R/hour}$$

APPENDIX g

The contribution from the third region is obtained using

$$\Delta I_3(1) = 0.142P \left\{ \frac{1 + 0.17\left[\frac{24-z}{25-z}\right]\sqrt{(25-z)^2+25}}{(25-z)^2+25} \right\} e^{-0.76\left[\frac{24-z}{25-z}\right]\sqrt{(25-z)^2+25} - .0943z} \Delta z \qquad (49)$$

Numerical integration yields

$$I_3(1) = 1.18\text{x}10^{-4}\ P \text{ R/hour}$$

Thus the intensity at h, a point one foot above the pool surface, and lying on the extended axis is

$$I(1) = 4.56P\text{x}10^{-3} \text{ Roentgens/hour} \qquad (50)$$

ORNL-LR-DWG. 2405
UNCLASSIFIED

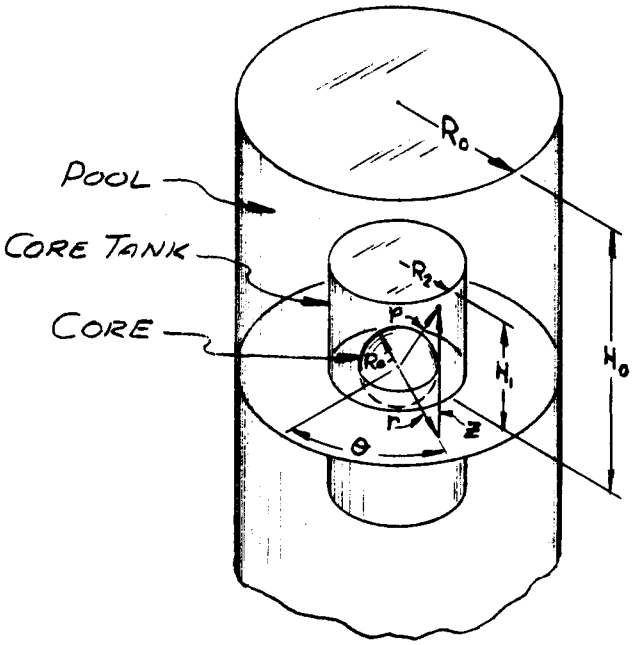

FIGURE-1

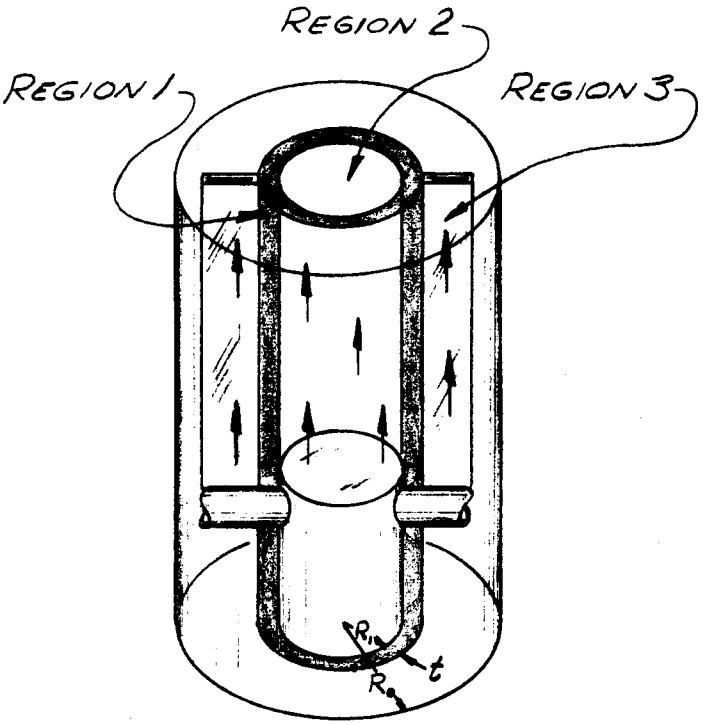

FIGURE-2

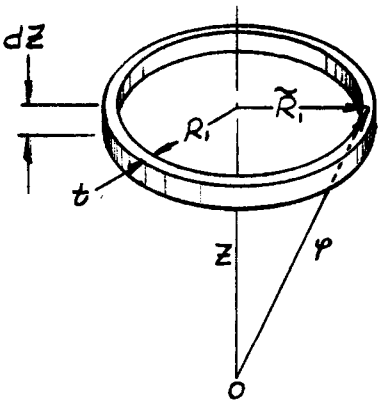

FIGURE-3

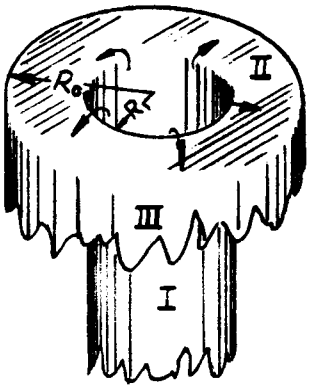

FIGURE-4

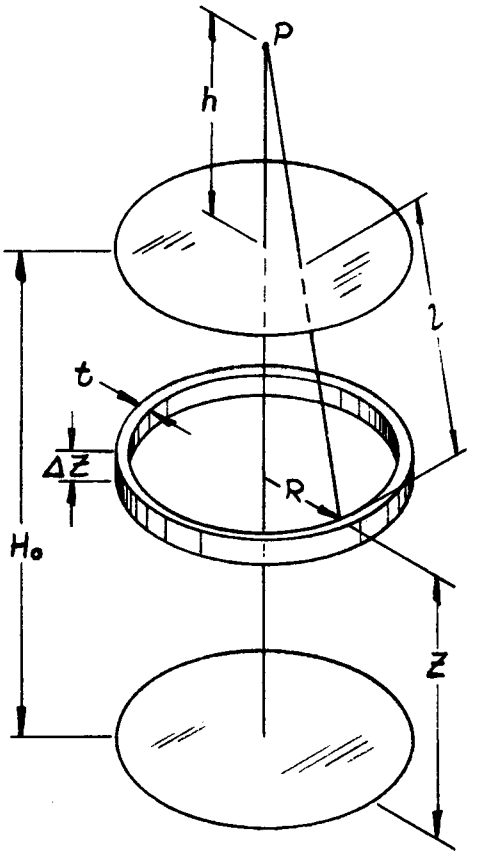

FIGURE-5

ORNL-LR-DWG. 2406
UNCLASSIFIED

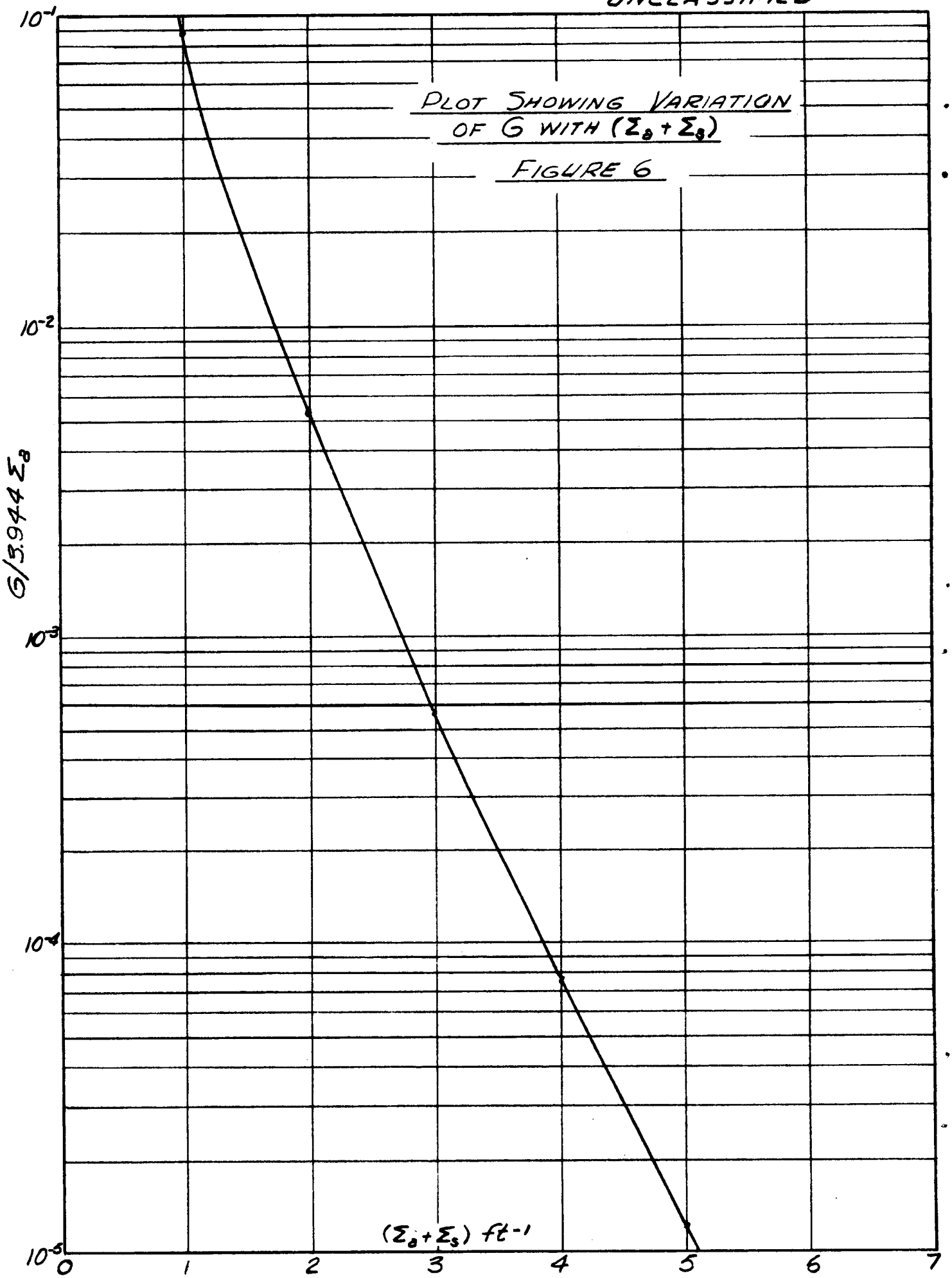

PLOT SHOWING VARIATION OF G WITH $(\Sigma_a + \Sigma_s)$

FIGURE 6

APPENDIX g

REFERENCES

1. R. G. Cochrane Private Communication

2. N. F. Lansing CF-54-4-170

3. B. E. Watt AECD-3073

4. R. S. Caswell WASH-152

5. R. G. Cochrane Private Communication

6. Paul & Clark Can J. Physics 31 267 (1953)

7. Huffman and Lenox ANL-EKF-44

APPENDIX h

OPERATING CONDITIONS OF THE ORR COOLING SYSTEM

J. P. Sanders

Introduction:

Calculations have been made according to the methods outlined in CF 53-3-57* to determine the minimum velocities which must be maintained in the ORR fuel assemblies. Inlet reactor water temperature of 100°, 120°, and 140°F, and total operating power of 5, 10, and 30 megawatts have been investigated.

Maximum Heat Flux:

Calculations have been made by R. B. Briggs ** to determine the maximum heat flux which can be expected in a MTR type assembly at various operating power levels. These calculations are based on data reported for the Materials Testing Reactor in IDO-16047-PPCo.***

In this report,*** the thermal neutron flux distribution in the fuel assemblies and beryllium L-pieces for the MTR is given at two different operating conditions. One determination, designated as Run No. 3, was for a fully depleted reactor condition; that is, the shim-safety rods were almost completely withdrawn. The other determinations, designated as Runs No. 5 and No. 1, were made for a clean, cold reactor condition; that is, the beryllium shim-safety rods were fully withdrawn and the fuel shim-safety rods were approximately 17 inches withdrawn.

---

* Sanders, J. P. "Heat Transfer and Pressure Loss in Proposed ORR Fuel Assemblies," ORNL-53-3-57, March 11, 1954.

** Personal Communciations with R. B. Briggs.

*** Bright, G. O. and Schroeder, F., "Neutron Flux Distributions in the Materials Testing Reactor," Part I, IDO-16047-PPCo, February 16, 1953.

APPENDIX h

The determinations of neutron flux were made by an activation method using lengths of cobalt wire inserted in the assemblies. The results were reported as a plot of the relative activity in the cobalt wire at positions correlated with a vertical traverse of the reactor. These values of relative activity may be converted to thermal neutron flux by multiplying by 3.9×10^{14} for Run No. 3 and by multiplying by 6.8×10^{14} for Runs No. 1 and No. 5. In all runs an additional correction factor of 0.87 must be used in the fuel section to correct for the activation of the wire due to epi-cadmium neutron contributions.

An examination of the plots of activity as a function of vertical position in the reactor indicated that the highest peak flux in the fuel assemblies for Run No. 5 occurred in assembly designated C-36. This peak flux corresponded to a relative activity of 0.72; therefore, the thermal flux was

$$0.72 \times 0.87 \times 6.8 \times 10^{14} = 4.25 \times 10^{14} \text{ neutrons/cm}^2\text{-sec.}$$

For Run No. 3, the maximum peak activity was found in fuel assembly designated C-35. The activity was 0.82; therefore, the thermal flux was

$$0.82 \times 0.87 \times 3.9 \times 10^{14} = 2.78 \times 10^{14} \text{ neutrons/cm}^2\text{-sec.}$$

For Run No. 3, the peak activities were read from the plot for each of the 23 fuel assemblies. An average of these readings showed that the average peak activity for the 23 fuel assemblies was 0.64. The average peak flux for these assemblies is

$$0.64 \times 0.87 \times 3.9 \times 10^{14} = 2.17 \times 10^{14} \text{ neutrons/cm}^2\text{-sec.}$$

APPENDIX h

If it can be assumed that these flux distributions for Run No. 3 can be represented by a sine curve symetrical about the center line of the reactor and having a value of 0.4 times its maximum at the upper and lower edges, the ratio of the peak flux in any assembly to the average flux is found as

$$\frac{\int_{\sin^{-1}\phi = 0.4}^{\pi/2} \sin\phi \, d\phi}{\frac{\pi}{2} - (\sin^{-1}\phi = 0.4)} = 1.28$$

Each of the plates of the fuel assemblies has 0.96 square feet of surface. For a 19-plate assembly this is equal to 18.2 square feet of heat transfer surface per assembly. For 30 megawatt operation with 27 assemblies the average heat flux is

$$\frac{30,000}{27} \times \frac{1}{18.2} \times 3,413 = 208,000 \text{ Btu/hr-ft.}^2$$

The average of the peak heat fluxes is

$$208,000 \times 1.28 = 267,000 \text{ Btu/hr-ft.}^2$$

The highest peak heat flux for Run No. 3 is

$$267,000 \times \frac{2.78 \times 10^{14}}{2:17 \times 10^{14}} = 342,000 \text{ Btu/hr-ft.}^2$$

Also, by conservative estimation, the highest peak heat flux obtained at start-up (Run No. 5) is

$$267,000 \times \frac{4.25 \times 10^{14}}{2.17 \times 10^{14}} = 522,000 \text{ Btu/hr-ft}^2$$

or approximately 600,000 Btu/hr-ft.^{2}

The foregoing calculations are based on a power level of 30 megawatts with 27 assemblies. In order to apply this information to 5 megawatt operation, it is assumed that the number of assemblies used is 20.

APPENDIX h

Thus average heat flux is

$$\frac{5{,}000 \times 3414}{20 \times 18.2} = 46{,}900 \text{ Btu/hr-ft.}^2$$

and the highest peak flux obtainable is

$$46{,}900 \times 1.28 \times \frac{2.78 \times 10^{14}}{2.17 \times 10^{14}} = 76{,}800 \text{ Btu/hr-ft.}^2$$

An additional factor of 1.3 is used to account for any peaking of the flux at the edges of the assemblies next to the beryllium. This factor is about equal to the distortion of flux found at start-up at the higher power levels. This distortion will not be present at the lower power levels because of the decrease in excess k necessary to over ride the xenon poisoning. Thus the maximum heat flux expected at a power level of 5 megawatts is

$$76{,}800 \times 1.3 = 100{,}000 \text{ Btu/hr-ft.}^2$$

Interpolating between the values of 600,000 Btu/hr-ft^2 for 30 megawatt operation and 100,000 Btu/hr-ft^2 at 5 megawatts, a maximum heat flux of 200,000 Btu/hr-ft^2 is estimated as a conservative value for 10 megawatt operation.

Inlet Water Temperatures:

Calculations were made for inlet water temperatures to the reactor of 100°, 120°, and 140°F. These were assumed to include the range of operation for systems operating either with Dricoolers (heat exchangers using atmospheric air as the coolant) or spray towers.

There is a desire to use a high inlet water to the reactor pursuant with good operational and design characteristics in order to minimize the difficulty of transferring the heat load to the atmosphere. Opposing this desire is the increased flow rate through the assembly necessary to maintain the liquid in contact with the plates at sub-boiling temperatures.

APPENDIX h

This increase in flow rate is evident from an examination of Figure No. 1 and No. 2 of this report.

Minimum Water Velocity Through Assembly:

With these maximum heat fluxes and inlet water temperatures established, the minimum water velocity necessary to maintain specified maximum surface temperatures in the fuel plates can be calculated. The method used was that developed and illustrated in CF 54-3-57.* The results of these calculations are shown graphically in Figures No. 1 and 2 of this report.

Total Flow in Reactor:

For a 19-plate assembly the flow area per assembly was calculated to be 0.0426 square feet. As a conservative estimate, the number of assemblies which would be used was assumed to be 27. Thus the total flow in the fuel assemblies is 516.8 V gallons per minute where V is the velocity in the assemblies in feet per second. In addition 20% was added to this total to account for the flow in the reflector pieces.

In Table I, the minimum velocity, as read from Figures No. 1 and No. 2 of this report and Figure No. 3 of ORNL CF 54-3-57**, is given for the indicated maximum power levels and inlet water temperatures. Maximum allowable surface temperatures of 200, 210, 220, and 230°F are assumed. The pressure losses in the assemblies are read from Figure No. 1, ORNL CF 53-3-57.***

---

* Sanders, J. P., op. cit.

** ibid, p. 21

*** ibid, p. 12

ORNL-LR-DWG.-489

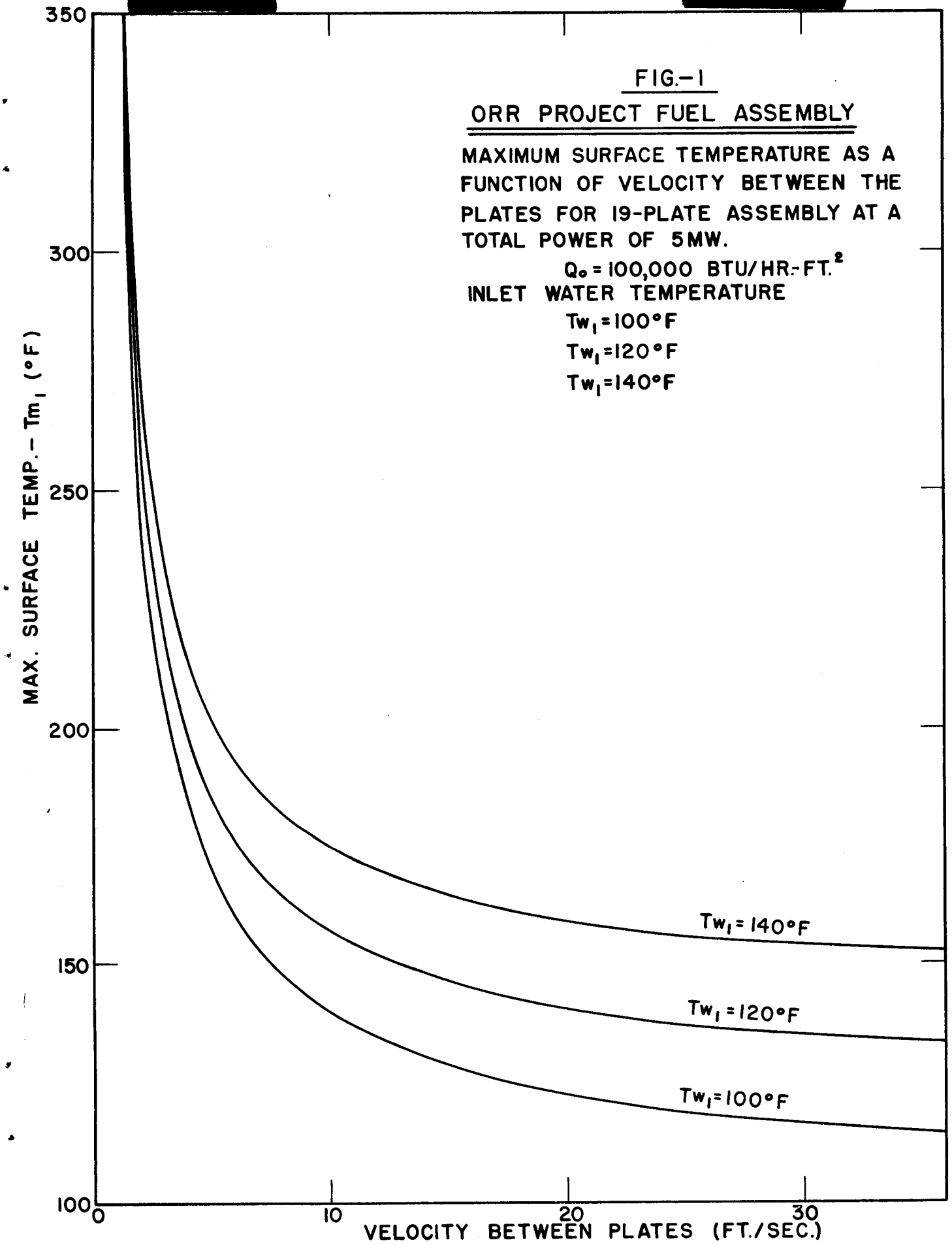

[redacted] ORNL-LR-DWG.-490 [redacted]

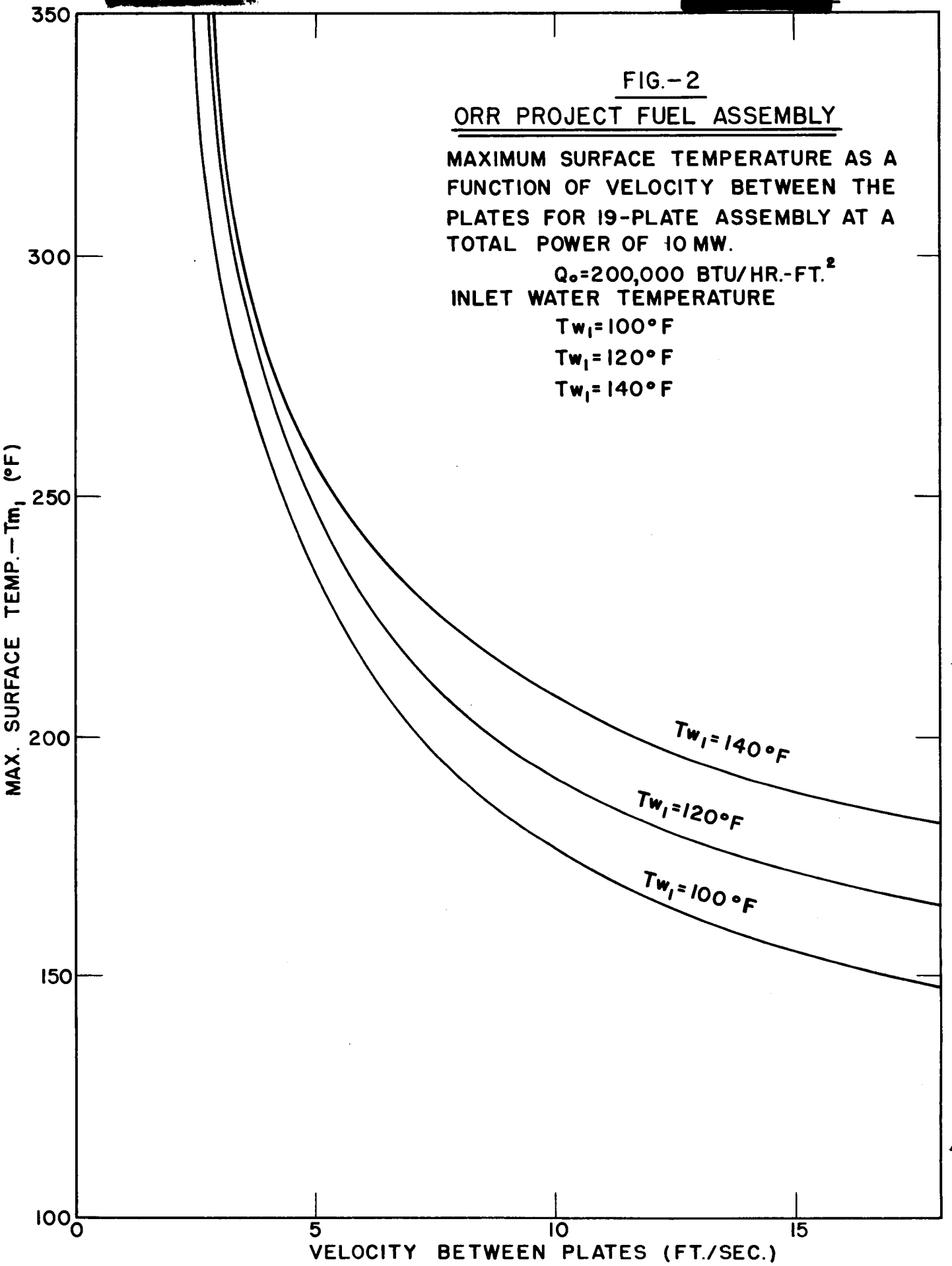

TABLE I

APPENDIX h

Total Flow Rates

For 27 19-Plate Assemblies

Power (M W)	Inlet Water Temp. (°F)	Max. Surface Temp. (°F)	Minimum Water Velocity (ft./sec.)	Pressure Loss (psi)	Flow for 27 Ass'y (gal./min.)	Change in Water Temp. T (°F)
5*	100	230	2.2	0.2	1292	26.6
		220	2.5	0.3	1469	23.4
		210	2.8	0.4	1645	20.9
	120	230	2.6	0.3	1528	22.5
		220	2.9	0.4	1704	20.2
		210	3.3	0.5	1938	17.7
		200	3.8	0.7	2357	14.6
	140	230	3.2	0.5	1879	18.3
		220	3.6	0.6	2114	16.3
		210	4.2	0.8	2467	14.0
10**	100	230	5.2	1.3	3054	22.5
		220	5.7	1.5	3348	20.5
		210	6.4	1.8	3760	18.3
	120	230	6.0	1.6	3524	19.5
		220	6.6	2.0	3877	17.8
		210	7.6	2.5	4464	15.4
		200	8.7	3.2	5400	12.7
	140	230	7.1	2.2	4170	16.5
		220	8.3	2.9	4876	14.2
		210	9.8	4.0	5756	12.1
30***	100	230	19.0	14.2	11,160	18.5
		220	21.1	17.6	12,396	16.6
		210	23.6	21.5	13,862	14.9
	120	230	21.8	18.8	12,804	16.1
		220	24.6	23.4	14,450	14.3
		210	28.2	30.3	16,665	12.4
	140	230	26.2	26.3	15,390	13.4
		220	30.0	34.3	17,622	11.7
		210	35.1	46.3	20,617	9.9

* ($Q_o = 10^5$ Btu/hr-ft^2)

** ($Q_o = 2 \times 10^5$ Btu/hr-ft^2)

*** ($Q_o = 6 \times 10^5$ Btu/hr-ft^2)

APPENDIX h

The overall change in water temperature in passing through the assemblies was made from a simple heat balance

$$5.69 \times 10^4 H = 8.29 G Cp \Delta T.$$

Where 5.69×10^4 is the power in Btu/minute which is equivalent to 1 megawatt, H is the reactor power in megawatts, 8.29 is the density in pounds per gallon at 100°F, G is the total flow rate in gallons per minute, Cp is the specific heat of water which is 1 Btu/pound - °F, and ΔT is the temperature change of water in °F. For the various power levels this is

For 5 MW

$$\Delta T = \left(\frac{3.434 \times 10^4}{G}\right)$$

For 10 MW

$$\Delta T = \left(\frac{6.868 \times 10^4}{G}\right)$$

For 30 MW

$$\Delta T = \left(\frac{20.61 \times 10^4}{G}\right).$$

Design Conditions for the ORR:

The ORNL Research Reactor is to be designed to operate at 5 megawatts. The inlet water temperature has been selected as 120°F. This selection is based on the proven operating characteristics of the LITR in this temperature range. As an additional safety factor the maximum allowable surface temperature has been fixed at 200°F. With these design criteria, the flow rates can be established from data in Table I. The flow through the reactor is 2500 gallons per minute, the temperature rise is 13.7°F and the pressure loss due to friction in the lattice is 0.8 psi.

APPENDIX h

If at some future date the power level were extended to 10 megawatts, and the same design conditions were desired, the flow rate would be 5,500 gallons per minute, the temperature rise would be 12.5°F and the pressure loss in the lattice would be 3.3 psi.

APPENDIX i

To: The File

Date: September 28, 1954

EXPERIMENT REVIEW COMMITTEE

An Experiment Review Committee, responsible to the Research Director, has functioned for several years in examining all experiments proposed for insertion in the Graphite Reactor and the LITR. Each experiment is checked for general operability with special attention being given to hazards to the reactor and personnel.

The procedure follows the general pattern of a detailed proposal, submitted by the experimenting group, preliminary and final reviews followed by a written report to the Research Director.

Membership of the committee of five includes physicists, chemists and engineers experienced in reactor operation, in-pile experimentation and reactor controls.

(Signed) E. P. Epler
Chairman Experiment Review Committee

APPENDIX i

[redacted]

REACTOR OPERATION REVIEW COMMITTEE

To: T. E. Cole

Date: September 27, 1954

The Reactor Operations Review Committee (RORC) was established on June 16, 1953 to review the operations of the reactors at ORNL. This Committee attempts to determine whether the operation of these ractors presents a hazard to the personnel of the Laboratory or the surrounding population. The Committee does not attempt to review new reactors before they are put into operation; this is a function of the Reactor Safeguards Committee and local design review committees. The RORC is more concerned with the day-to-day operation of the reactors; that the operational procedures are safe and are being adhered to; that the maintenance of safety equipment is adequate. In addition the Committee is called upon to pass on proposed changes in procedures or equipment.

(Signed) W. H. Jordan
Chairman Reactor Operation Review Committee

[redacted]

[redacted]

[redacted]

APPENDIX j

INTER-COMPANY CORRESPONDENCE

OAK RIDGE NATIONAL LABORATORY
CARBIDE AND CARBON CHEMICALS CORPORATION
Post Office Box P
Oak Ridge, Tennessee

To: Memo

Date: August 26, 1954

Copy To: E. E. Beauchamp
F. T. Binford
T. E. Cole
J. A. Cox
J. H. Gillette
Eugene Lamb
R. V. McCord
P. B. Orr
M. E. Ramsey (2)
E. J. Witkowski

Subject: RADIOISOTOPE PRODUCTION IN THE RR

After the RR starts routine operations (winter, 1956-57), radioisotope production irradiations will be started and maintained at a level which will not interfere with research work. It is questionable whether we will also continue to operate the graphite reactor and LITR; this matter will be discussed more fully in another memorandum. Operation of the other reactors will have some bearing on radioisotope production requirements in the RR, but for the purposes of this discussion we will assume that only the RR is operated.

Radioisotope production is now divided among the various AEC reactors as follows.

X-Reactor - Irradiation Units
Services Irradiations (e.g., piston rings)
Sulfur for P^{32}
Uranium Slugs for I^{131}
Gold for Au^{198} and Hg^{198} (Length Standard)
Sb-Be Neutron Sources
Low Specific Activity Ca^{45}
Co^{60} Needles
Short-lived Fission Products, separated and mixed.

Hanford - Co metal for Co^{60} (intermediate specific activity, large volume)
Be_3N_2 for C^{14}
KCl for Cl^{36} and S^{35}
High Specific Activity, long-lived isotopes (e.g., Ag^{110}, Zn^{65}).

[redacted]

[redacted]

[redacted]

APPENDIX j

Memo August 26, 1954

MTR - Co Metal for high specific activity Co^{60}
High specific activity, intermediate half-life radioisotopes (e.g., Ca^{45}, Sc^{46}, Cd^{115}, Sn^{113}).

LITR - Special Service Irradiations (requiring higher flux than X-Reactor)
High Specific Activity short-lived to intermediate half-life radioisotopes (e.g., Na^{24}, Fe^{59}, Cr^{51}).

The initial operation of the RR will probably be at 5 megawatts and all of the flux figures given here are based on this power level. Since the power will probably be raised shortly to 10 megawatts, we can reasonably hope to double the flux within a year after operation starts.

The lattice of the RR according to present plans will be 9 X 7 , with the fuel occupying a space 4 X 6 . Around the lattice on three sides will be a single row of beryllium reflector pieces, while on one (west) side there will be two rows of beryllium reflector pieces. Actually, some of these beryllium reflector pieces on the west side can be replaced by special cans containing sulfur and general purpose irradiation stringers similar to those in the LITR. For iodine production, uranium slugs in baskets can be irradiated in beryllium reflector pieces (all of which have a removable 2" core piece); special cooling will be required for this. A sketch of the presently proposed lattice is attached.

Sulfur for P^{32} Production

The space available in the reflector will be approximately 3" X 3" X 24", or 216 cubic inches, compared to approximately 150 cubic inches in the present sulfur can. At 5 megawatts, we should have in the sixth row next to the fuel a thermal flux of 3×10^{13} n/cm^2/sec, compared with a maximum flux of 10^{12} in the graphite reactor. Since we maintain about 26 cans in the graphite reactor, or about 3750 cubic inches, and we will have an advantage of 30 in the thermal flux (and higher in the fast flux), we should need for equivalent production 3750/30 = 125 cubic inches. Therefore, it will be necessary to use only one stringer with cans about 3" square X 6" long which could be inserted inside an aluminum shell.

Irradiation of U Slugs for I^{131}

Slugs for iodine production can be irradiated in a beryllium reflector piece with approximately a 2"-diameter hole. Six 4" slugs in a basket will be irradiated in each beryllium piece. The position in the seventh row of the lattice will have a flux of 2×10^{13}, compared with

[redacted]

[redacted]

APPENDIX J

Memo August 26, 1954

the graphite reactor, where we now use 16 slugs per week at a flux of about 8×10^{11}. We should have an advantage in the RR of $2 \times 10^{13}/8 \times 10^{11} = 25$. Assuming we use one slug per week and left each slug in for 14 weeks, we would require approximately two stringers.

General Purpose Stringers

We now have 199 samples in stringers 13 and 14 of the X-Reactor, plus about 50 in the LITR. Using the LITR type of stringers, we will be able to handle about 65 samples per stringer. At the higher flux in the RR, this is quite adequate. It is estimated that about three stringers would be required. These would be in the seventh row in a flux of about 2×10^{13}.

Irradiation of Large Samples

There is a large space in the west side of the lattice where samples could be irradiated in a flux of about 1×10^{13}; however, these samples would have to be placed in water-tight cans. After the irradiation is completed, the cans could be moved to the radioisotope area for disassembling.

Rabbit Tubes

There are now two pneumatic and two hydraulic tubes planned. The size of the pneumatic rabbits will be the same as those of the LITR, while the hydraulic rabbits will be considerably larger, 1" - 1½" in diameter. The exact location of the rabbit tubes has not yet been determined, but depending upon their location they should be in a flux of 1 or 2×10^{13}.

In general, it appears that we could produce in the RR everything that is needed for the radioisotope program except large amounts of Co^{60}, Au^{198} and C^{14}. Of course, we may find some space eventually for production of some of these materials, but it is not recommended because it would be a waste of valuable RR neutrons and space. The X-Reactor is convenient for inserting miscellaneous large objects for irradiation because it is air-cooled and loading is relatively simple. Operation of the graphite reactor would also take some of the load off the RR.

Depleted fuel elements from the LITR are now sent to Arco for processing. With proper scheduling, this processing could be done in the Thorex plant, thereby saving time, money, SF transfers, and provide excellent feed for the proposed Fission Product Plant.

[redacted]

[redacted]

[redacted]

APPENDIX j

Memo

August 26, 1954

With the RR in operation, we will make only limited use of other reactors, as follows.

Hanford (or Savannah, if feasible)

Co^{60}
Be_3N_2 for C^{14}
KCl
Special long-term irradiations.

X-Reactor, LITR

Not operating.

MTR

Special high specific activity Co^{60}
A few irradiations requiring 10^{14} flux.

RR

All other irradiations.

Other feed material for the radioisotope program would be fission product wastes from Hanford, Savannah, possibly Arco, ORNL pilot and metal recovery plants; mint from Hanford; mint daughter from Los Alamos; Kr^{85} crude F.P. gas from Arco.

It has been suggested by J. A. Cox that those Be locations to be occupied by special isotope stringers (such as sulfur cans and iodine slugs) be established early in the construction period so that expensive Be pieces need not be purchased for these locations. He further suggests that since we have a Be allotment we seldom use, some Be for the RR might be purchased against it, with other than RR funds during the next two years.

A. F. Rupp

AFR:jml

[redacted]

APPENDIX j

[redacted]

[redacted]

O	O	O	O	O	O	O	O	O
O	F	F	Shim	F	Shim	F	F	O
O	F	F	F	F	F	F	F	O
O	F	F	Shim	F	Shim	F	F	O
O	F	F	F	F	F	F	F	O
O		S		O	O	O	O	O
O	O Iodine	O	O Iodine	O	G	O	G	O

18" Beam Hole

Large 18" Beam Holes

Space for Large Irradiations

F — Fuel

O Iodine — 6 Slugs for Radio-iodine Production

S — 6 Sulfur Cans

G — General Purpose Stringer - 65 cans

O — Beryllium With 2" Core Piece

[redacted]

APPENDIX k

PROPOSED ANP EXPERIMENTS IN THE ORR

L. P. Meem

The design group for the ORR has requested a description of the type of experiments that might be inserted in one of the large access facilities in the ORR by the ANP Project. Numerous informal discussions were held six months ago and earlier between representatives of ANP, the ORR, and the Solid State Division on the type of experiments proposed. These proposals are summarized in this memorandum. It should be recognized that the proposed experiments are subject to considerable modification as more information is obtained from experiments in the LITR and MTR. Also, the more complex experiments can probably be omitted since the 60 Mw CFRE has now been approved on a 4-year basis.

A need was recognized early in the discussions for a much larger access hole to the high flux region of the reactor than is now available in other reactors. This large facility has been provided in the design of the ORR and it will be possible to operate large equipment such as a full-size aircraft circulating fluoride pump in the facility.

Obviously, the first few experiments placed in the reactor will be much more modest in scale and will be modeled along the present fuel loop in the LITR.[1] However, the large access hole has been designed so that it would be physically possible to insert a fuel loop capable of generating on the order of 1 megawatt of power with a power density on the order of 1000 watts/cc. Such a loop would provide high flux, high ΔT, and high flow in one experiment. A full-size aircraft type pump would be used and a large heat exchanger would be required to dissipate the heat.

With such a facility available, the following are some of the problems which could be investigated:

I. Mechanical Equipment

1. Radiation heating and distortion

2. Endurance of equipment under combined radiation and temperature conditions

---

1. Brundage, Parkinson, and Sisman, Questionnaire for LITR Fluoride Fuel Loop Experiment, CF 53-12-140.

APPENDIX k

3. Effect of radiation on pump lubricant

4. Fission gas leakage from pump

5. Chemical compatibility of bearings with radiation.

II. Nuclear and Control

1. Xenon purging

2. Fission product gas disposal.

III. Chemistry and Metallurgy

1. Fuel system mass transfer

2. Fuel system corrosion

3. NaK system mass transfer

4. NaK system corrosion

5. Chemical stability of fuel at high burnup

6. Reducing effect of fission at high burnup

7. Na-Be-Inconel compatibility.

The answers to all of the above problems could not be obtained in a single experiment, but would come from a series of experiments. In general, each experiment would have a core section in which nuclear power would be produced, a pump to circulate the fuel, and a heat exchanger to absorb the power. The simpler type experiments will be performed first and as succeeding experiments become more complicated re-evaluation and coordination with the CFRE program will be required.

APPENDIX 1

REACTOR MECHANICAL CONTROLS

J. P. Gill

In the early stages of design for the ORNL Research Reactor, it had become apparent that a number of advantages could be realized in locating the mechanical controls to operate from below the reactor, namely;

1) The control drive system is permanently located and need not be removed for fuel reloading operations or inspection.

2) During the critical experiments, and normal reloading, safety rods will be in a position for operation.

3) Reactor and control components are brought closer together and during installation are aligned and referenced from a single machined surface in the reactor structue. Misalignment due to repeated removal of controls is eliminated.

4) Additional space is made available above the core for vertical experiments.

Early in 1952, these principals of operation of controls were incorporated in the design specifications for the ORNL Research Reactor, and a program was initiated to develop a suitable safety drive and release mechanism which did not sacrifice any of the safety or serviciability requirements of the MTR type design. During the design and preliminary stages of testing, interest in a similar control arrangement by North American Aviation, for the UPR, resulted in a combined effort which has satisfactorily developed a design suited to the needs of both reactor programs.

The shim rod drive and release mechanism design showing the most promise was incorporated in the design of ORR and a prototype of the system was built at the Y-12 Plant of ORNL to test the installation under simulated reactor operating conditions. A ball bearing trigger, a push rod to actuate the balls, and an electromagnet constituted the release device, as illustrated in Figure 9 and 9a. The ball bearing trigger which directly supports the shim rod is held in the cocked position by a push rod. The magnet armature holds the push rod up against the force of a 175# spring; thus a failure of the magnet current results in a scram.

After a number of modifications to the initial installation, under full water flow condition, release times of both the mechanical and electrical systems were measured during a simulated life test of over 3000 cycles. During this period, in which there were no indications of release mechanism failure, the mechanical release time in each case was under 18 milliseconds. Laboratory tests on a magnet designed specifically for this installation show a maximum of 8 milliseconds delay, thus a total release delay of approximately 25 milliseconds can be expected. As the ORR Project has progressed in the last few years, a number of changes and modifications in the reactor design, with probable improvements, requires that a new prototype of the system be tested. This work is now in progress and a full report will be available soon after completion of the tests.

Reference Report: 1) ORNL-CF-53-11-25, Release Time Investigation for the ORR Shim Rods.

2) ORNL-Dwg. No. F-17920, Test Installation Assembly

[redacted]

DWG. No. 21690
[redacted]

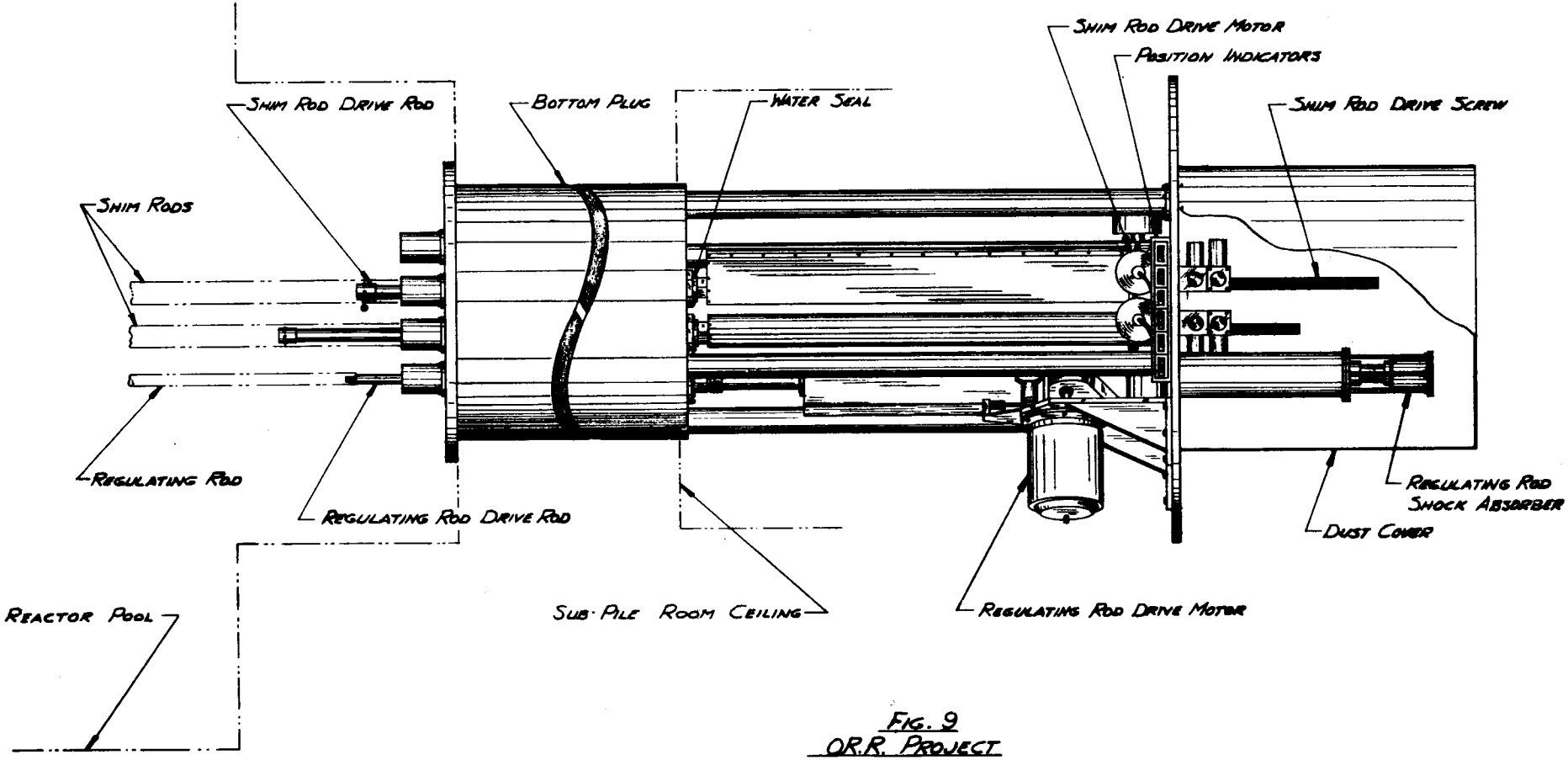

FIG. 9
O.R.R. PROJECT
CONTROL DRIVES ASSEMBLY

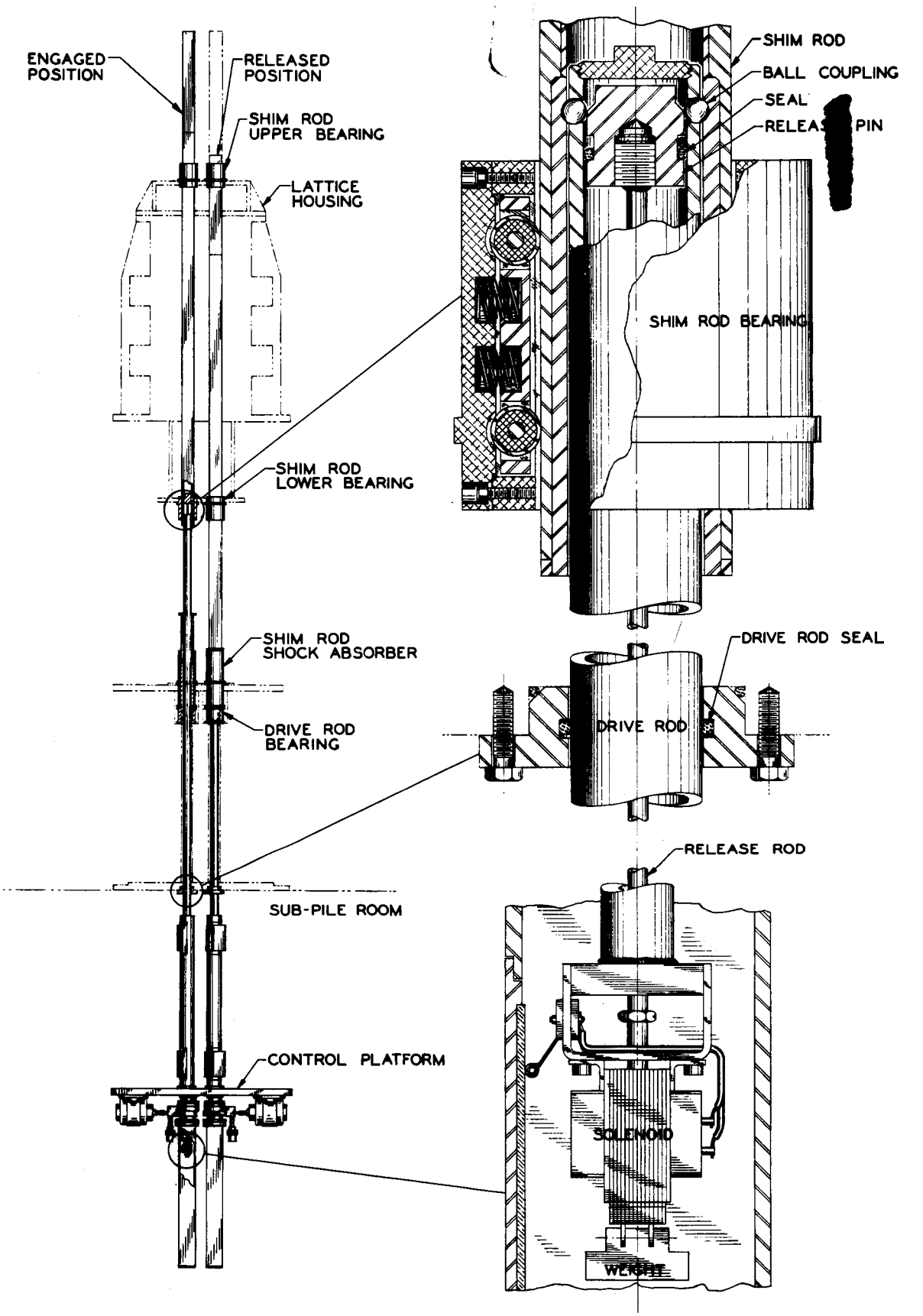

ORNL RESEARCH REACTOR
SHIM ROD RELEASE MECHANISM

SK-123 [redacted]

Fig. 9a

APPENDIX m

DISPERSION OF AIRBORNE WASTES IN THE X-10 AREA

U. S. Weather Bureau - Oak Ridge, Tennessee

September 1954

1. Introduction:

Due to the fact the site of the ARE is only 0.75 miles from the site of the ORR, data previously obtained in connection with the ARE project is here presented as being typical of the conditions prevailing at the ORR site.

Observations of wind speed and direction measured at a height of 70' at the site of the proposed ARE are combined with wind, temperature gradient and rainfall measurements made at the X-10 Health Physics Division and elsewhere in the Oak Ridge Area and with winds aloft measured at nearby Weather Bureau stations to show the climatology of the site.

Specialized measurements of the turbulence, wind speed gradients and temperature gradients are used to make quantitative estimates of the meteorological factors involved in the travel and dilution of contamination released deliberately or accidentally at the site of the proposed ARE.

2. Stability of the lower layers of the atmosphere:

The lower layers of the atmosphere tend to be more frequently stable than unstable with inversions (constant or increasing temperature with height) occurring about 56% of the time annually. Fall is usually the season with the greatest percentage of hours with inversions and summer, as might be expected, is the season with the least number of hours of inversions. A summary of the seasonal percentage of frequency of inversions as measured at X-10 Health Physics is shown in Table I for the period 1944-53.

APPENDIX m

Table I

Frequency of inversions ($T_{183}' - T_4'$)

	1944	1945	1946	1947	1948	1949	1950	1951	1952	1953	Avg.
Winter	43.4	43.1	53.1	64.4	55.1	43.8	68.2	74.6	46.9	51.9	54.5
Spring	45.4	45.0	55.7	M	54.9	58.9	58.4	83.9	40.9	49.7	54.8
Summer	44.1	52.5	50.4	52.8	41.1	57.1	59.5	50.2	49.8	66.9	52.4
Fall	51.1	65.5	55.7	61.4	33.4	67.9	80.5	52.8	46.0	61.2	57.6
Annual	46.0	51.5	53.7	59.2	46.1	56.9	66.5	65.4	45.9	57.4	54.8

A frequency distribution of the $T_{183}' - T_4'$ temperature gradient (Fig. 1) shows the smallest range of values in the summer and fall with a greater range in spring and winter. Higher wind speeds in winter and spring tend to increase the percentage of neutral or adiabatic lapse rates (dashed vertical line) during these seasons.

Figure 1 also shows the distribution of temperature gradient between the surface and the 850 millibar pressure level (approximately 5000' MSL). The stability is much more pronounced in the deep layer of air than in the 200' layer above the ground. A marked shift occurs during the spring from the very stable winter to the slightly stable distribution in the summer. By fall, the transition to the stable winter pattern begins. It should be noted that the frequency of adiabatic or neutral lapse extending through the whole layer up to 5000' MSL is not large.

Low level soundings taken at 03000E, 0900E, 1500E and 2100E from the summer of 1949 through the Fall of 1950 are summarized in figure 2. The average temperature gradients of the lowest 1000 feet are the most affected by

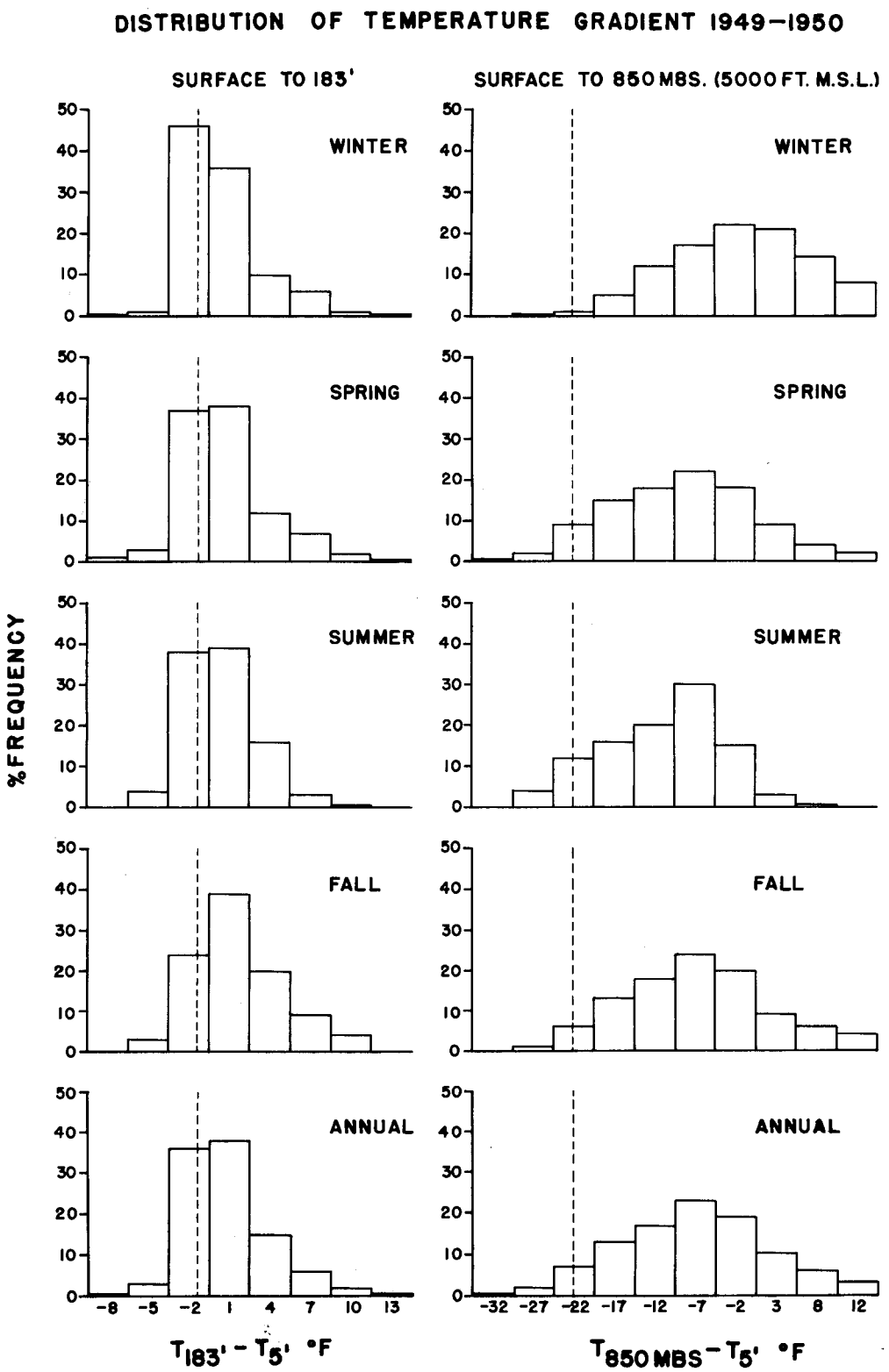
DISTRIBUTION OF TEMPERATURE GRADIENT 1949–1950
SURFACE TO 183'
SURFACE TO 850 MBS. (5000 FT. M.S.L.)
WINTER
SPRING
SUMMER
FALL
ANNUAL
% FREQUENCY
0
10
20
30
40
50
-8 -5 -2 1 4 7 10 13
-32 -27 -22 -17 -12 -7 -2 3 8 12
T183' - T5' °F
T850 MBS - T5' °F

Fig. 1

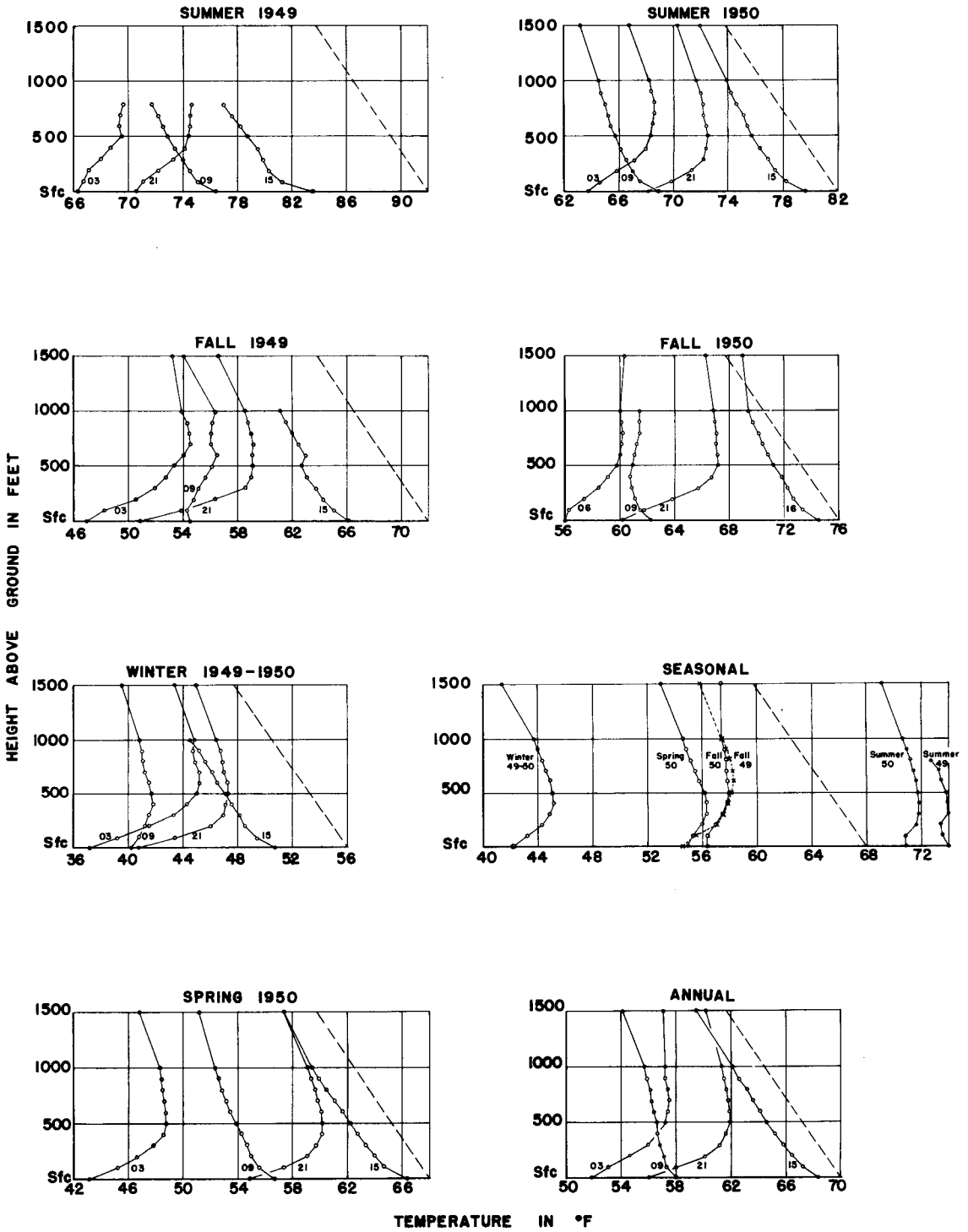
SUMMER 1949
SUMMER 1950
FALL 1949
FALL 1950
WINTER 1949-1950
SEASONAL
SPRING 1950
ANNUAL
HEIGHT ABOVE GROUND IN FEET
TEMPERATURE IN °F
1500
1000
500
Sfc
Winter 49-50
Spring 50
Fall 50
Fall 49
Summer 50
Summer 49

Fig. 2

diurnal changes. The nocturnal inversion is well developed in the 0300E and 2100E soundings. This inversion which forms after sunset usually builds up to 400-800 feet with the stable layer extending higher, often to 5000 feet.

The afternoon temperature gradients as shown by the 1500E soundings are very unstable in the lowest 100 feet and usually are neutral or slightly unstable to several thousand feet.

As to the implications of these climatological conditions it is expected that any contaminant emitted into the inversion layer at ambient temperature will not be mixed vertically, but will remain at or near its level of emission with a minimum of dilution, while a contaminant emitted into an unstable layer will be mixed through the unstable layer in a comparatively short time during which puffs of relatively high concentration may be momentarily brought to the ground.

3. Winds in relation to stability:

The valleys in the vicinity of the site are oriented NE-SW and considerable channeling of the winds in the valley might be expected. This is evident in Figure 3 which shows the annual frequency distribution of winds at the stations in the vicinity of X-10 operated during the Meteorological Survey. The prevailing directions are up-valley winds from the SW and WSW with a secondary maximum of down-valley winds from the NE and ENE. These prevailing wind regimes reflect the orientation of the broad valley between the Cumberland Plateau and the Smokey Mountains as well as the orientation of the local ridges and valleys. The gradient wind in this latitude is usually SW or westerly and so the day time winds tend to reflect a mixing down of the gradient winds. The night winds represent drainage of cold air down the local slopes and the broader

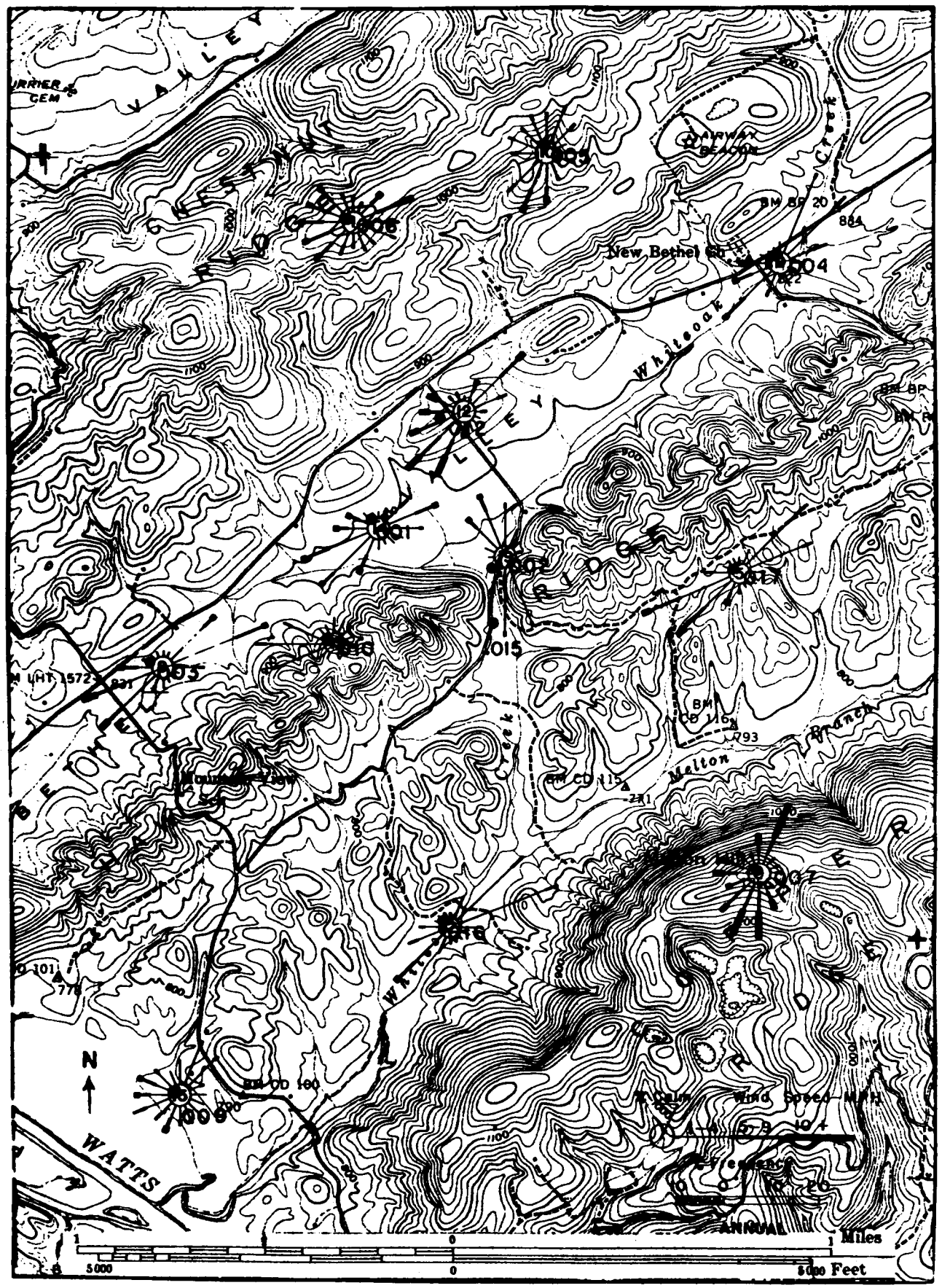
New Bethel Ch
Whiteoak
Melton
Branch
Mountain View
WATTS
N
Wind Speed MPH
ANNUAL
Miles
Feet

Fig. 3

Tennessee Valley. The combination of these two effects as well as the daily changes in the pressure patterns over this area, give the elongated shape of the typical wind rose at a channeled valley station.

During inversions, the NE and ENE winds occur most frequently, usually at the expense of the SW and WSW winds. Many of these drainage winds are very light and are below the starting speed of the anemometer available. This characteristically increases the percentage of calms recorded during the night under stable conditions. It may be seen in Figure 4 that the percentage of calms is much higher under stable conditions at the X-10 area than under unstable conditions. The predominence of light NE and ENE winds under stable conditions is particularly marked in the summer and fall when the lower wind speeds aloft and the smaller amount of cloudiness allow the nocturnal drainage patterns to develop.

In Figure 4, the unstable wind roses are typical of the daytime conditions when turbulence and dilution are most pronounced. Wind speeds under these conditions are usually above average. The stable wind roses are typical of night time when lower wind speeds, little turbulence and a minimum of dilution are observed.

It should be noted that the higher frequency of calms at X-10 in 1951 was caused by the starting speed of 2-3 mph for the generator anemometer at the location whereas the older X-10 instrument had a starting speed of under 1 mph.

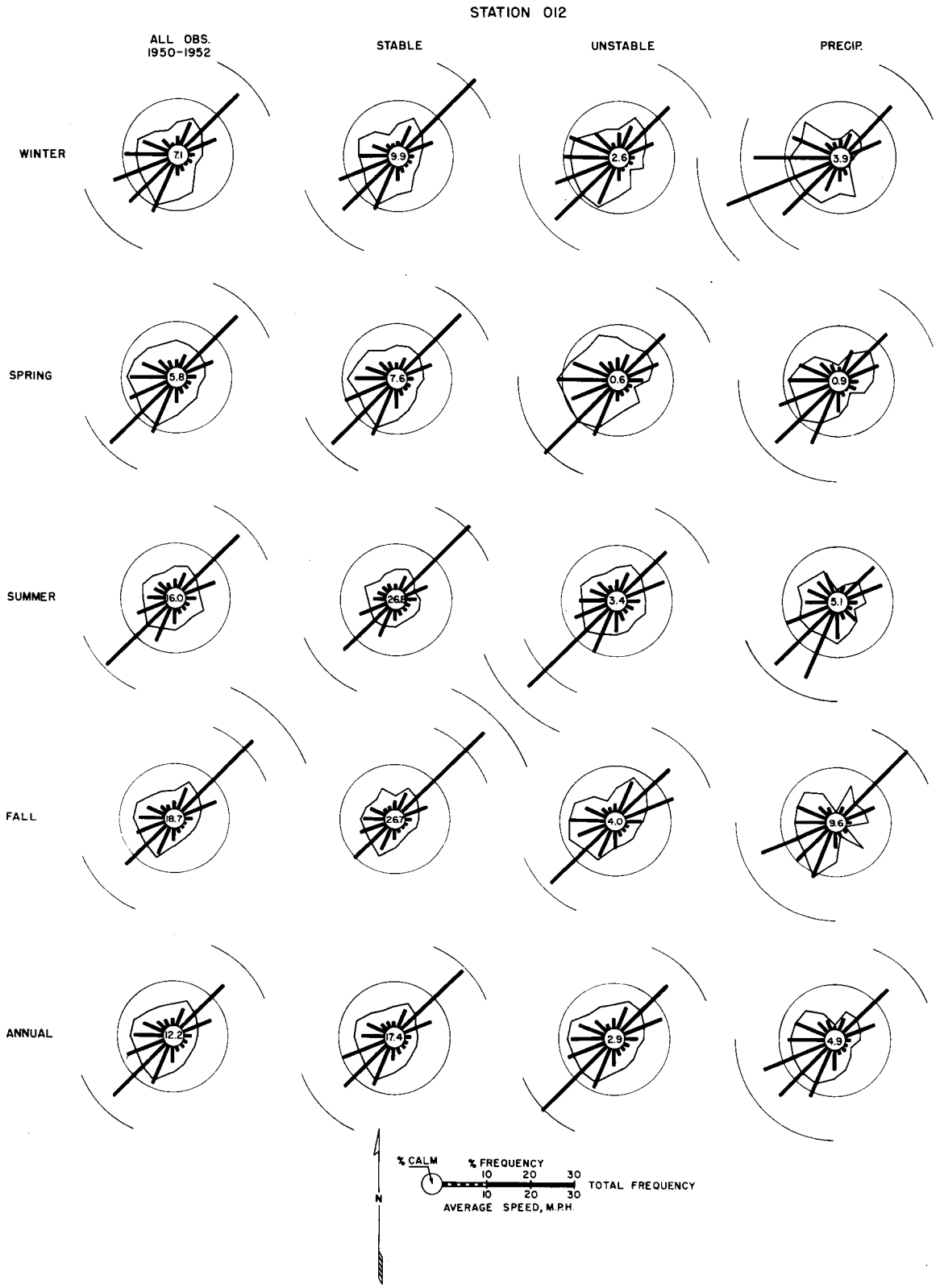
STATION 012
ALL OBS. 1950-1952
STABLE
UNSTABLE
PRECIP.
WINTER
SPRING
SUMMER
FALL
ANNUAL
7.1
9.9
2.6
3.9
5.8
7.6
0.6
0.9
6.0
26.8
3.4
5.1
18.7
26.7
4.0
9.6
12.2
17.4
2.9
4.9
N
% CALM
% FREQUENCY
10 20 30
10 20 30
TOTAL FREQUENCY
AVERAGE SPEED, M.P.H.

Fig. 4

Table II

Annual Frequency of Wind Direction

	X-10 (1951)	X-10 (1944-1950)		
	All obs.	Stable	Unstable	All obs.
Calm	12%	3%	1%	2%
NNE	4	4	4	4
NE	18	17	12	18
ENE	9	11	10	9
E	1	3	5	4
ESE	1	4	5	3
SE	1	2	4	3
SSE	1	3	4	3
S	2	2	2	2
SSW	9	9	7	8
SW	14	12	16	15
WSW	11	11	8	9
W	6	7	9	8
WNW	6	7	6	6
NW	2	2	4	3
NNW	1	2	1	2
N	2	1	1	1

The seasonal distribution of average hourly wind speed for 1951 is shown in Table III.

APPENDIX m

Table III

Average Hourly Wind Speed MPH (1951)

X-10 Area (140')

	Winter	Spring	Summer	Fall	Annual
Stable	5.4	6.1	2.1	2.9	4.4
Unstable	7.1	9.3	5.2	5.7	6.1
All Obs.	6.0	6.6	3.7	4.3	5.1

4. Local variation in the wind:

Considerable variation is observed both in wind speed and direction within small distances in Bethel Valley and Melton Valley. A study of the wind flow patterns which occur during the warm and cold halves of the year with several groups of stability in the lowest 5000' under various regimes of 5000' wind direction and speed were made. All the hourly wind observations from the stations operated during the meteorological survey of 1949-50 were sorted by these parameters and the prevailing direction for each station was plotted.

Examples of the effects of these parameters on the local winds in the vicinity of X-10 are illustrated in figures 5 and 6. These wind patterns are typical of the winter or cold half of the year when vegetative cover is at a minimum and the surface is less sheltered from the winds aloft. Station 010 was located within the tree cover on Haw Ridge and is typical of the travel of contaminants released at low levels on a north facing slope. All four patterns shown in figure 5 occurred with the same wind direction at 5000' MSL, that is from the SW. In the daytime when the air is relatively

DAY-UNSTABLE

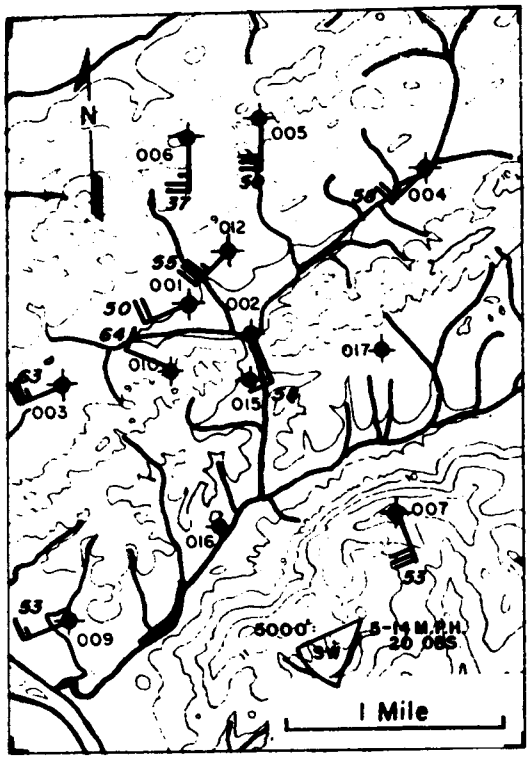

NIGHT-STABLE

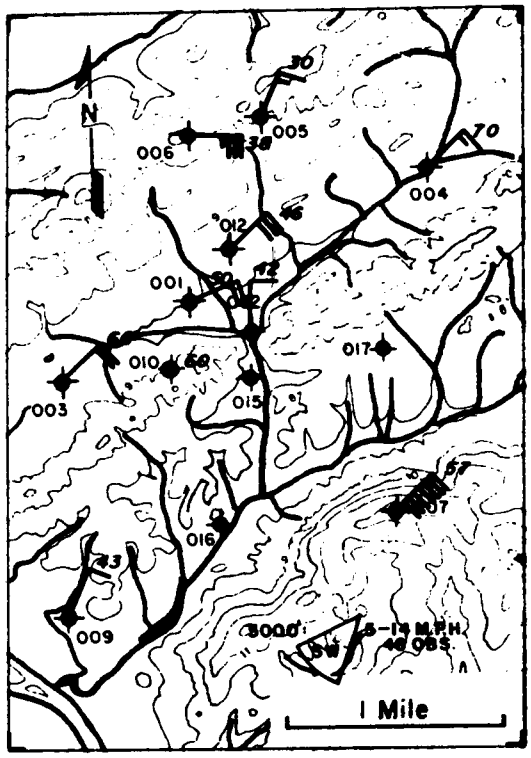

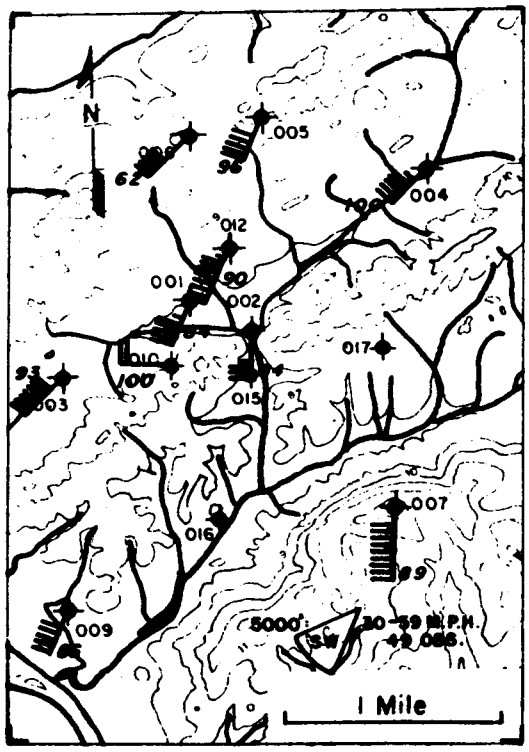

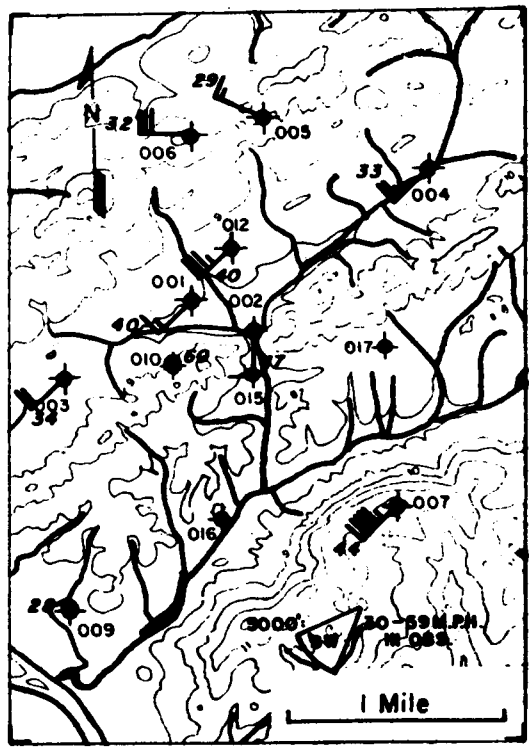

DIR: SSW
SPEED: 3 M.P.H.
FREQ: 62 %

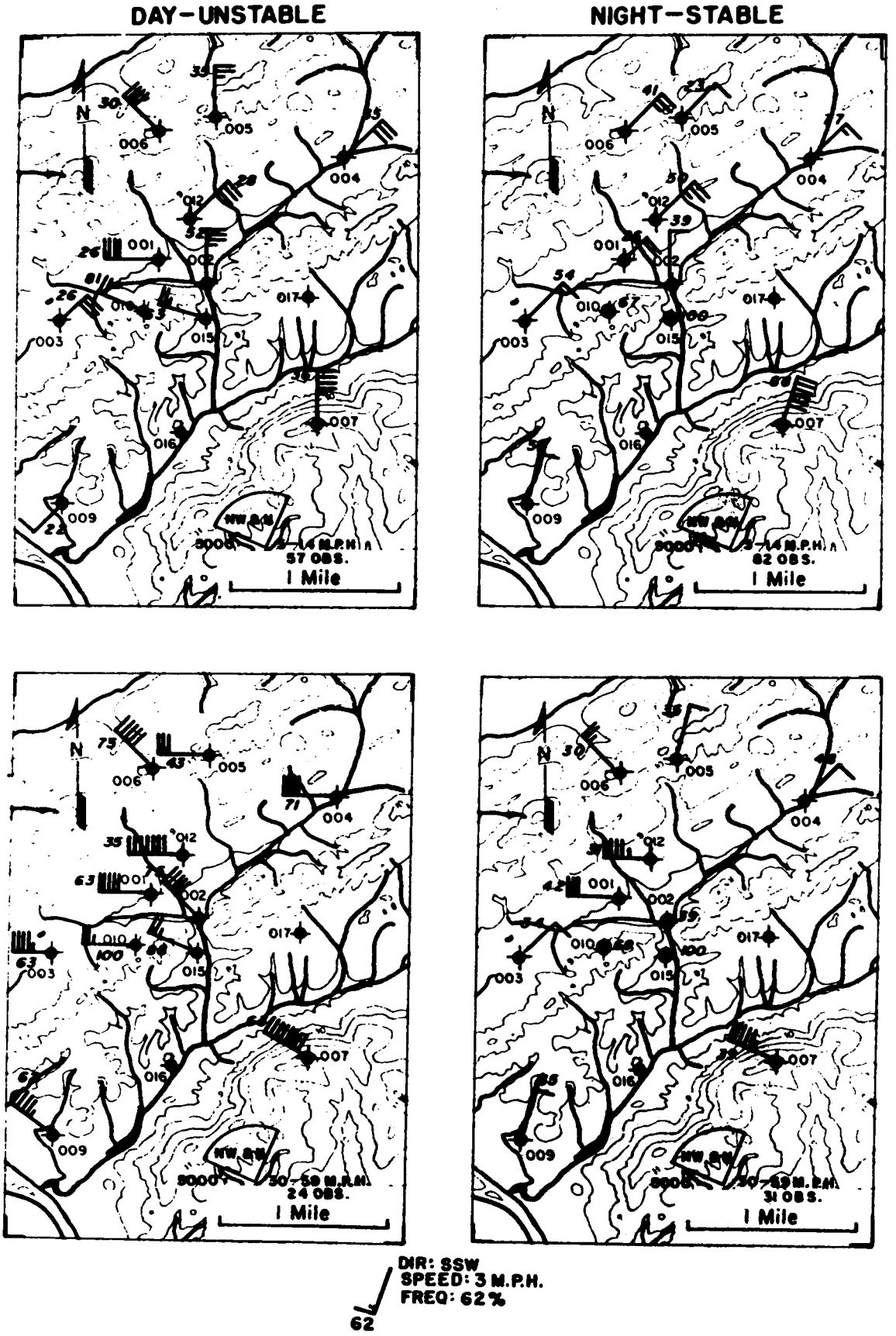
DAY-UNSTABLE
NIGHT-STABLE
N
001
002
003
004
005
006
007
009
010
012
015
016
017
3000'
3-14 M.P.H.
57 OBS.
82 OBS.
24 OBS.
31 OBS.
1 Mile
DIR: SSW
SPEED: 3 M.P.H.
FREQ: 62%
62

Fig. 6

unstable through the 5000' layer, the local winds tend to follow the upper winds in direction. The degree with which they follow is determined mainly by the speed of the upper winds. With the 5000' winds ranging between 5 and 14 mph, direct up slope winds occur on Chestnut Ridge, but the valley stations follow closely. If the upper wind speed is increased to 30-59 mph, all the stations follow quite well except the station under the trees at Hawk Ridge.

During the night when the air is stable, and with light upper winds, the winds on the surface follow their own pattern of drainage of cold air from the local ridges down the local valley and the deeper current down the Tennessee Valley. If the wind speed in the upper layer is increased to 30-59 mph and all other parameters remain the same, the more exposed stations follow the SW wind and the percentage of calms increases considerably at most stations. The well protected stations have the drainage wind cancelled and their prevailing wind becomes calm. It is interesting to note that the wind velocity at Melton Hill (1431 MSL) is reversed from a drainage wind of 14 mph to a gradient wind of 11 mph during the night merely by an increase of the upper wind from light to strong.

In figure 6, the effect of cross ridge gradient winds from the N and NW at 5000' MSL is shown under the same combinations of speed and stability as in figure 5. Here again, even with the upper winds blowing across the ridges, the valley stations tend to follow the gradient winds in day time with a fidelity dependent on the speed of the upper wind. It should be noted, however, that the probability of the wind following the prevailing direction is smaller for the cross valley wind than the up-valley wind. Under stable conditions at night, down-valley flow again predominates when

the upper winds are light and at right angles to the valley orientation. When the upper wind speed is strong, the surface winds tend to follow it except at sheltered locations where the prevailing wind is generally calm or at least below the starting speed of our anemometers.

Generalizing from these examples and others which have been studied, we may say that in night time or in stable conditions, the winds tend to be generally NE and ENE and rather light in the valley regardless of the gradient wind, except that strong winds aloft will control the velocity and direction of the valley winds, reversing them or producing calms when opposing the local drainage. In the daytime, the surface winds tend to follow the winds aloft with increasing reliability as the upper wind speed increases. Only with strong winds aloft or winds parallel to the valley would it be of value to attempt to extrapolate air movements for any number of miles using valley winds. In the well developed stable situation, however, a very light air movement will follow the valley as far downstream as the valley retains its structure, even though the prevailing winds a few hundred feet above the ground are in an entirely different direction. In general, air transport from a valley location will be governed by the local valley wind regime and the degree of coupling with the upper winds.

5. Upper winds:

A comparison of the pibal observations made throughout 1949-50 at Knoxville and Oak Ridge shows that above about 2000 feet, the wind roses are almost identical at these two stations. This identity in the data makes possible the use of the longer period of record (1927-50) from Knoxville to eliminate the abnormalities introduced by the use of the short record at Oak Ridge.

APPENDIX m

Annual wind roses are shown for Knoxville (1927-1950) and Nashville (1937-1950) in figure 7. pibal observations are only made when no low clouds, dense fog or precipitation is occurring and so are not truly representative of the upper wind at all times. Three years of Rawin data for Nashville (1947-1950) are available consisting of observations taken regardless of the current weather at the time of observation. A comparison of these wind roses for Knoxville and Nashville shows that the mode for winds above 3000 meters MSL should be shifted to westerly instead of a WNW when observation with rain are included in the set. In summer and fall, the winds aloft are lightest and the highest winds occur during the winter months at all levels.

Table V shows the annual frequency and speed of the wind aloft for Knoxville for several representative levels.

Table V

Annual Frequency of Wind Direction and Average Speed, Knoxville (1927-50)

	500m MSL		1500m MSL		3000m MSL	
Direction	%	mph	%	mph	%	mph
Calm	1		0		0	
NNE	6	10	5	12	4	14
NE	10	10	4	12	3	13
ENE	9	10	3	12	2	12
E	4	7	2	10	2	11
ESE	2	6	2	8	1	11
SE	2	6	2	9	2	11
SSE	2	8	2	12	2	12
S	4	10	5	17	2	14
SSW	7	13	10	23	3	18
SW	20	15	15	24	5	22
WSW	12	12	13	21	9	25
W	7	12	12	20	12	26
WNW	4	11	9	17	16	28
NW	3	8	7	15	16	28
NNW	3	9	6	14	13	23
N	5	10	5	13	7	18
Average Speed		11		18		23

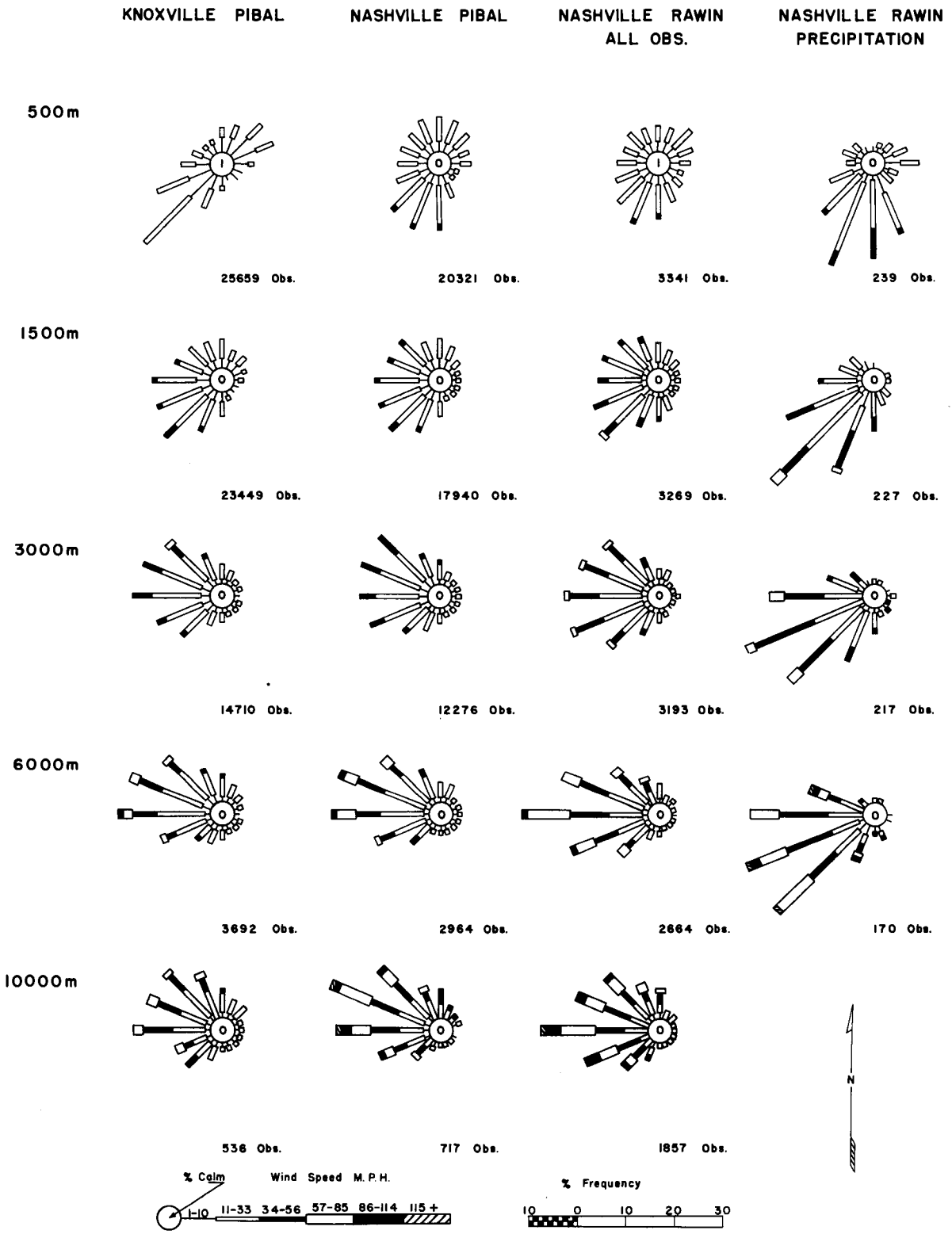
KNOXVILLE PIBAL
NASHVILLE PIBAL
NASHVILLE RAWIN ALL OBS.
NASHVILLE RAWIN PRECIPITATION
500m
25659 Obs.
20321 Obs.
3341 Obs.
239 Obs.
1500m
23449 Obs.
17940 Obs.
3269 Obs.
227 Obs.
3000m
14710 Obs.
12276 Obs.
3193 Obs.
217 Obs.
6000m
3692 Obs.
2964 Obs.
2664 Obs.
170 Obs.
10000m
536 Obs.
717 Obs.
1857 Obs.
N
% Calm
Wind Speed M.P.H.
1-10
11-33
34-56
57-85
86-114
115+
% Frequency
10
0
10
20
30

Fig. 7

APPENDIX m

The NE-SW axis of the valley between the Cumberland Plateau and the Smokies continues to influence the wind distribution over the Tennessee Valley up to about 5000', although the variations within the Valley do not extend above about 2000'. Above 5000' the Southwesterly mode gives way to the prevailing westerlies usually observed at these latitudes.

6. Correlation of Winds with Precipitation

Figure 4 contains a wind rose for the surface wind at X-10 using only the hours of observation in 1950 and 1951 during which precipitation was measured. The direction distribution is very little different from that of all observations. This is consistent with the experience of precipitation forecasters that there is little correlation between surface wind direction and rain, particularly in rugged terrain. Figure 7 shows the upper winds measured at Nashville during the period 1948-50 when precipitation was occurring at observation time. In general the prevailing wind at any given level is shifted to the SW or SSW from W or SW and the velocity somewhat higher during the occurrence of precipitation, with the shift being most marked in the winter.

APPENDIX m

Table VI

Annual Frequency of Wind Direction and Average Speed with Precipitation Occuring

	Knoxville Sfc. (1950-51)		Nashville Rawin 1500m MSL		3000m MSL	
Direction	%	mph	%	mph	%	mph
Calm	6		0		0	
NNE	3	4	0		1	13
NE	16	6	0		0	
ENE	6	4	1	16	1	7
E	1	4	1	21	1	11
ESE	1	2	0		1	36
SE	1	3	2	24	1	20
SSE	1	4	3	19	1	12
S	4	6	8	28	5	26
SSW	10	8	17	32	12	26
SW	16	8	28	31	22	37
WSW	13	8	17	30	25	38
W	9	8	9	27	18	39
WNW	7	7	6	21	8	27
NW	3	7	4	22	4	33
NNW	2	4	2	5	1	16
N	1	1	1	7	1	18
Average Speed		5		28		34

The average number of days with 0.01 in. of precipitation is 139 annually with January having the highest average. The maximum days with rain in one month was 22 in January of 1950. September and October are the months with the least number of days with precipitation, averaging 7 each.

MAKE-UP OF SURROUNDING AREA

APPENDIX n

Table 1 lists the total number of persons employed at each plant within the AEC restricted area, but no attempt has been made to indicate the number of workers on each shift. However, practically all these employees work a 40-hr week. Table 2 lists the surrounding towns with a population of 500 or more, and Table 3 gives the rural population by counties. Table 3 was originally prepared for the ARE hazards report,[1] but the two facilities are located in the same area (ORR is 0.75 mi southeast of the ARE) and there would be little if any variation in the figures. Figure 21, also originally presented in the ARE hazards report, shows the surrounding counties and all towns with a population greater than 500. In this figure it should be noted that the radii of the circles are measured from the ARE site, rather than from the ORR site.

A list of vital industrial and defense installations within a 30-mi radius is given in Table 4.

(1) Aircraft Reactor Experiment Hazards Summary Report, ORNL 1407 (Nov. 24, 1952).

[redacted]

DWG. 17019

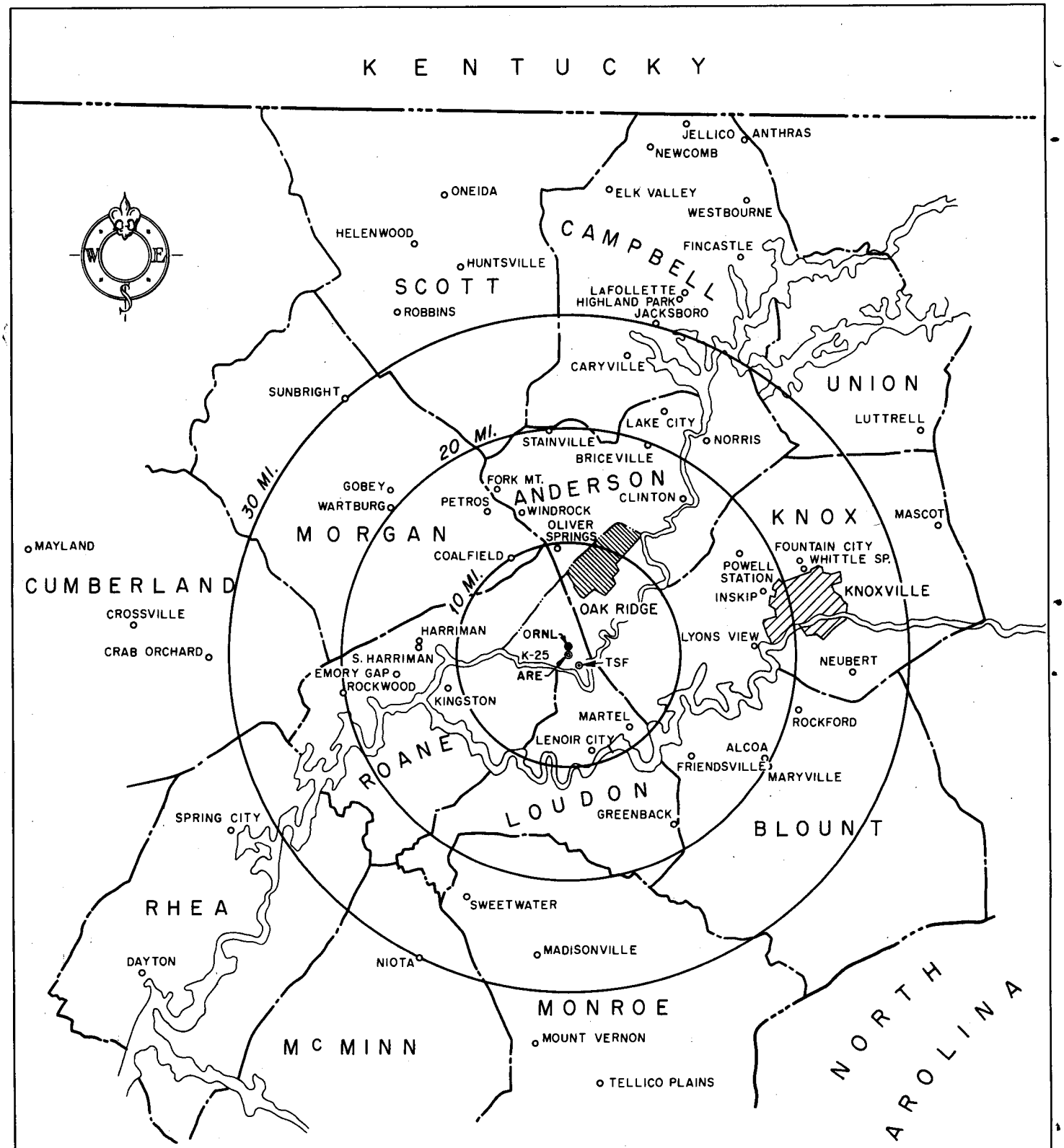

FIG. 21.

MAP OF COUNTIES

SURROUNDING OAK RIDGE AREA

APPENDIX n

Table 1. Personnel within AEC Restricted Area

Plant	Distance from ORR (mi)	Direction	No. of Employees
Homogeneous Reactor Experiment	0.75	SSE	20
Aircraft Reactor Experiment	0.75	S by E	75
Tower Shielding Facility	1.75	SE by S	10
Gaseous Diffusion Plants (K-25, -27, -29, -31, -33)	5.5	WNW	6128 CCCC 5672 Construction
Electromagnetic Plant (Y-12)	5.5	NE by N	4100

APPENDIX n

Table 2. Population of Surrounding Towns[a]

City or Town	Distance from ORR (mi)	Direction	Population
Oak Ridge	6 - 13	N by E	30,229
Martel	7	SE	500
Lenoir City	7.5	S by E	5,159
Oliver Springs	9.5	N by W	1,089
Coalfield	10.	NW by N	650
Kingston	11.5	W by S	1,627
Friendsville	12.5	SE by E	600
Windrock	14.5	NNW	550
Harriman	14.5	W by N	6,389
South Harriman	14.5	W by N	2,761
Petros	16	NW by N	790
Emory Gap	16	W	500
Lyons View	16	E by N	500
Greenback	16.5	SE by S	960
Fork Mountain	17	NNW	700
Clinton	17	NE by N	3,712
Powell Station	17	NE by E	500
Knoxville	17 - 24	E by N	124,760
Inskip	18	ENE	685
Alcoa	19.5	ESE	6,355
Maryville	20	ESE	7,742
Rockford	20	E by S	950
Briceville	20	NNE	885
Wartburg	21	NW	800
Stainville	21	N by W	500
Rockwood	20	W	4,272
Whittle Springs	22	ENE	675
Fountain City	22	ENE	11,500
Gobey	23	NW	513
Norris	23	NE by N	1,134
Sweetwater	23	SSW	4,199
Lake City	24	NNE	1,827
Neubert	24	E	600
John Sevier	26	E by N	752
Madisonville	26	S	1,487
Caryville	28	N by E	1,234
Niota	29	SW by S	956

(a) Towns within a 30-mile radius that have a population of 500 or more.

APPENDIX n

Table 3. Rural Population in the Surrounding Counties

County	Total Area (sq mi)	Rural Population Density (a) (No. of people per sq mi)	Population Within 0- to 10-mi Radius	Population Within 10- to 20-mi Radius	Population Within 20- to 30-mi Radius
Anderson	338	62[b]	310	10,850	6,700
Blount	584	67	0	6,840	25,000
Campbell	447	48	0	0	6,240
Cumberland	679	22	0	0	1,760
Knox	517	178	9,780	24,900	37,000
Loudon	240	54	3,780	7,940	1,240
McMinn	435	39	0	0	2,690
Meigs	213	29	0	0	1,160
Monroe	665	26	0	910	5,510
Morgan	539	22	195	3,165	4,620
Rhea	335	33	0	0	1,720
Roane	379	50[b]	4,650	9,250	2,950
Scott	549	26	0	155	2,890
Union	212	38	0	0	570
			18,715	63,910	100,050

(a) Includes all county population except communities with population of 500 or more.

(b) Does not include Oak Ridge area.

APPENDIX n

Table 4. Vital Industrial and Defense Installations within a 30-mi Radius

Industry or Installation	Distance from ORR (mi)	Direction
Homogeneous Reactor Experiment	0.75	SSE
Tower Shielding Facility	1.75	SE by S
Aircraft Reactor Experiment	0.75	S by E
Gaseous Diffusion Plants (K-25, -27, -29, -31, -33)	5.5	WNW
Electromagnetic Plant (Y-12)	5.5	NE by N
Fort Loudon Dam	8	SSE
Kingston Steam Plant (TVA)	12	W
Assorted Small Industries in Knoxville	17 - 24	E by N
Aluminum Company of America	18	ESE
McGhee-Tyson Airport	18	ESE
Air Force Radar Station, Lake City	24	NNE

APPENDIX o

SELECTED RADIATION HAZARDS OF O.R.R.

T.H.J. Burnett

Summary

A maximum permissible exposure to the bones and/or thyroid of 25 rem would result from the inhalation of 470 μc of a mixture of 30 fission product isotopes. There would be present 4.4×10^6 curies of this mixture after 82 days operation at 5* megawatts. The total integrated dose downwind should not exceed 0.94 curie sec. per m^3. External dose associated with such an inhalation exposure would be negligibly small.

Introduction

The following discussion is grouped under three headings:

1. Selected Basis of Hazard
2. Criteria of Hazard
3. Excluded Hazard
4. Basis for Calculations
5. Methods of Calculation
6. Dosage Values and Inhalation Limits

1. Selection Basis of Hazard

We define a major reactor accident as one involving the release and airborne dispersion of part or all of the fission products accumulated in its fuel.

The external radiation exposure received from fission products passing aloft as a cloud, deposited on the ground, or thru the side of a building in which they are contained is readily measured. Some ORNL personnel with their film containing security badges are distributed at all times in the surrounding communities. Where external exposure alone is

*Twice this value would be present with operation at 10 megawatts power level for 82 da. The permissible exposure will not change.

involved, the levels at which various degrees of damage occur are relatively well known, and their hazard can be appraised. The calculations of probably external exposure associated with such dispersion are limited by the accuracy with which meteorological factors and the quantities and energies of radiation can be estimated.

When personnel are surrounded by airborne active material their inhalation intake and retention leads to an internal exposure to the lungs, G.I. tract, and other organs in addition to whatever external exposure is received. This internal exposure persists long after the transient external exposure has ceased and exceeds the external exposure by a large factor. For these reasons, and the difficulty of measuring it, internal exposure has been selected for detailed consideration.

2. Criteria of Hazard

It is generally considered that a total exposure of 25 rem may be received under emergency conditions once in a lifetime by adults without medically observable direct harm. There is more question about allowing a general population including young children to receive this exposure and ordinarily a reduction by a factor of ten is recommended. Following a single inhalation incident the total exposure to the less radiosensitive lungs, G.I. tract and thyroid is received over a period of time of the order of a few days, particularly if the activity is soluble. The exposure to the bones, however, is prolonged over a number of months. For this reason, we propose as the criteria for a general population that the permissible exposure shall not exceed 25 rem to the bone as the combined result of external

gamma during, and the total internal exposure following an inhalation intake. For the probable mixture of bone seeking fission product isotopes only one tenth of the internal exposure will be received by the bones during the first week and the concurrent total internal exposure to the lungs, G.I. tract, or thyroid should be no more than approximately 25 rem. While a greater exposure than this may be tolerated by the thyroid in adults it is unwise to exceed this level for children even in emergencies.

3. Excluded Hazards

No effort has been made to evaluate herein the hazards from probable external contamination of bodies, clothing, food, or terrain. Likewise, no evaluation has been made of possible special synergistic hazards due to simultaneous exposure of the lungs, G.I. tract, thyroid, and bones. No estimates have been made of internal exposure at times less than a few minutes since these will involve operating and laboratory personnel subject to other risk.

4. Basis for Calculations

Fission yields in ADE-65 by Hunter and Ballou were used for these preliminary calculations. It is intended to recheck this work using the most recent available fission yields reported in the literature (1) and given in a private communication from L. E. Glendenin, et al(2).

Decay schemes, half lives, and energy data were taken from the Table of Isotopes (Rev. Mod. Phys. 25, 469-651, April 1953) by Seaborg, et al.

Fractions of inhalation uptake, biological data, and equations for dosage calculations were taken from the ICRP report of Maximum Permissible Internal Dose (Revised Dec. 7, 1953), K. Z. Morgan, Chairman. Single intake

(1) PR 84, 860 (1951)
(2) ANL-OCS-383

dosage equations used were checked with the work of Morgan and Ford reported in Nucleonics, Vol. 12, No. 6, 32-39 (June 1954).

The reactor was assumed to have been operating 82 days at 5 megawatts in these preliminary calculations. While some shift in the relative amounts of different isotopes would occur with an increase in the operating time, this difference was felt to be small for the 115 days postulated for the ORR. It is planned to recalculate the amoumts of those isotopes chiefly affected and correct for this difference if justified.

Neutron capture by the fission products formed was neglected. No account was taken of isotopes in chains of very low yield nor of isotopes of short half life (those less than a few hours give small total dose).

5. Method of Calculation

A unit inhalation of one microcurie of a selected mixture of isotopes of interest was considered. This was taken as the mixture of fission products in the amounts of their relative abundances at time t= 0 after the incident as determined by the time of reactor operation. These isotopes were selected because their intermediate length of half life makes them of principal internal dose concern. Having half lives generally between 20 hours and 20 years the dosage produced are insensitive to decay in transit to the point of inhalation.

Based on retention and uptake values and the energies of the radiations, the dosages received by the bone, thyroid, and kidneys were calculated for the respective constituents of this mixture. The uptake considered was only to what is ordinarily considered the critical organ, i.e., no account was taken of the partial uptake to the kidneys of bone seeking elements, etc.

[redacted]

APPENDIX o

The total dosages produced by each isotope were calculated for several lengths of time after inhalation, 1 week, 13 weeks, 1 year, and 70 years. These dosages were then summed for the respective body organs affected. Using the summation dose to the bones (70 yr exposure case) from a unit inhalation, the total inhalation intake necessary to give the 25 rem permissible dose was then calculated.

Because of the non-uniformity of exposure factor, N = 5, for the bones, the corresponding transient dosage to the lungs and G. I. tract, otherwise controlling, appears to be comparable. A detailed calculation to check this point is planned.

A recheck of the iodine isotope dosages to the thyroid is planned since the effective energies used may in some cases have been based on external exposure.

6. Dosage Values and Inhalation Limits

The dosages to the bone, thyroid and kidneys following a unit inhalation are summarized in Table 1.

Table 1

Unit Intake* Exposures

Affected Body Organs	Initial Dose Rate mrem/day	Accumulated Total Dose			
		1st wk mrem	13 wks mrem	1 yr mrem	70 yrs mrem
Bone	1.35	5.42	26.5	38.3	53.1
Kidney[redacted]	0.16	0.47	1.1	1.1	1.1
Thyroid	33.42	33.75	50.8	50.8	50.8

*Inhalation of 1 μc of a mixture of 30 isotopes

A total dose to the bone of 25 rem is then seen to result from the inhalation of 470 μc of the mixture of fission products considered.

APPENDIX o

If a breathing rate of 30 l/min is assumed (= 5×10^{-4} m^3/sec), the maximum permissible exposure would be a total integrated dose not to exceed 0.94 curie seconds per cubic meter.

The 30 isotope mixture considered would be present to the extent of approximately 4.4×10^6 curies at t= 0 after reactor operation at 5 megawatts for 82 days.

The dose to the thyroid for the case of total release would be the same as in the case of escape of only the volatile fission products. Since it is prudent to limit thyroid exposure to the same 25 rem limit, corresponding dilution and total integrated dose values would apply. Thus, comparable hazards would exist at the same distance in the volatile fission product release case as for the total fission product release. The latter case, of course, would affect other organs in addition to the thyroid.

Subject to differences in power level and time of reactor operation, these results would apply to the HRT as well as to the ORR. The additional fission product activity produced during the power excursion phase of the reactor accident should be relatively small compared to the total present. It is planned to make supplementary calculations to evaluate this increment.